Virology 394 (2009) 64–72

Contents lists available at ScienceDirect

Virology

journal homepage: www.elsevier.com/locate/yviro

Selective infection of CD4$^+$ effector memory T lymphocytes leads to preferential depletion of memory T lymphocytes in R5 HIV-1-infected humanized NOD/SCID/IL-2Rγ^{null} mice

Chuanyi Nie [a,1], Kei Sato [a,1], Naoko Misawa [a], Hiroko Kitayama [a], Hisanori Fujino [b], Hidefumi Hiramatsu [b], Toshio Heike [b], Tatsutoshi Nakahata [b], Yuetsu Tanaka [c], Mamoru Ito [d], Yoshio Koyanagi [a,*]

[a] Laboratory of Viral Pathogenesis, Institute for Virus Research, Kyoto University, 53 Shogoinkawara-cho, Sakyo-ku, Kyoto, Kyoto 606-8507, Japan
[b] Department of Pediatrics, Graduate School of Medicine, Kyoto University, Kyoto, Kyoto 606-8501, Japan
[c] Department of Immunology, Graduate School of Medicine, University of the Ryukyus, Nishihara, Okinawa 903-0125, Japan
[d] Central Institute for Experimental Animals, Kawasaki, Kanagawa 216-0001, Japan

ARTICLE INFO

Article history:
Received 8 April 2009
Returned to author for revision 19 July 2009
Accepted 4 August 2009
Available online 9 September 2009

Keywords:
HIV-1 pathogenesis
Humanized mouse
Memory cell depletion
Productive infection
T cell activation

ABSTRACT

To investigate the events leading to the depletion of CD4$^+$ T lymphocytes during long-term infection of human immunodeficiency virus type 1 (HIV-1), we infected human CD34$^+$ cells-transplanted NOD/SCID/IL-2Rγ^{null} mice with CXCR4-tropic and CCR5-tropic HIV-1. CXCR4-tropic HIV-1-infected mice were quickly depleted of CD4$^+$ thymocytes and both CD45RA$^+$ naïve and CD45RA$^-$ memory CD4$^+$ T lymphocytes, while CCR5-tropic HIV-1-infected mice were preferentially depleted of CD45RA$^-$ memory CD4$^+$ T lymphocytes. Staining of HIV-1 p24 antigen revealed that CCR5-tropic HIV-1 preferentially infected effector memory T lymphocytes (T_{EM}) rather than central memory T lymphocytes. In addition, the majority of p24$^+$ cells in CCR5-tropic HIV-1-infected mice were activated and in cycling phase. Taken together, our findings indicate that productive infection mainly takes place in the activated T_{EM} in cycling phase and further suggest that the predominant infection in T_{EM} would lead to the depletion of memory CD4$^+$ T lymphocytes in CCR5-tropic HIV-1-infected mice.

Introduction

While it is evident that human immunodeficiency virus type 1 (HIV-1) causes acquired immunodeficiency syndrome (AIDS) in humans, the mechanism by which HIV-1 accomplishes this remains unclear. The gradual loss of peripheral blood (PB) CD4$^+$ T lymphocytes during the asymptomatic phase of HIV-1 infection is one of the best prognostic predictors for the onset of AIDS (O'Brien et al., 1996), and CD4$^+$ T lymphocyte depletion is thought to be a serious pathological change in AIDS (McCune, 2001).

To define the mechanisms behind CD4$^+$ T lymphocyte depletion, a large number of studies have been conducted in humans, primates, and humanized mice by using HIV-1, simian immunodeficiency virus (SIV), and SIV/HIV-1 chimeric virus (SHIV) (Centlivre et al., 2007; Koyanagi et al., 2008; McCune, 2001). One of the important findings from previous studies was the dependence of pathogenesis on the co-receptor preference, CXCR4, and/or CCR5 (Berkowitz et al., 1998; Moore et al., 2004). CXCR4-tropic (X4) SHIV caused rapid and complete depletion of all subsets of CD4$^+$ T lymphocytes in rhesus macaques, which led to death from immunodeficiency (Nishimura et al., 2004). On the other hand, CCR5-tropic (R5) HIV-1 is the dominant type of HIV-1 found in patients, and clinical manifestation of HIV-1 infection resembles CCR5-tropic SIV infection (Berger, Murphy, and Farber, 1999). In both HIV-1-infected patients and SIV-infected rhesus macaques, the drastic onset of immunodeficiency is rare (Ambrose et al., 2007; McCune, 2001), and CD4$^+$ T lymphocytes in PB slowly decrease in number, eventually leading to immunodeficiency.

X4 virus uses CXCR4 as the co-receptor and R5 virus uses CCR5 as the co-receptor for viral infection into target cells (Berger, Murphy, and Farber, 1999; Lusso, 2006). CXCR4 is expressed on naïve T lymphocytes and thymocytes, thus X4 HIV-1 can infect naïve T lymphocytes and thymocytes (Pedroza-Martins et al., 1998). It is well known that faster depletion of immature thymocytes and T lymphocytes is observed after the appearance of X4 HIV-1 (Berkowitz et al., 1998; Pedroza-Martins et al., 1998; Schnittman et al., 1990). On the contrary, CCR5 is primarily expressed on CD4$^+$ effector memory T lymphocytes (T_{EM}) and macrophages but not on naïve and central memory CD4$^+$ T lymphocytes (T_{CM}) (Sallusto, Geginat, and Lanzavecchia, 2004). Therefore, the selective infection of T_{EM} is thought to leave naïve T lymphocytes and T_{CM} intact. Depletion of T_{EM} by R5 virus has been studied in SIV-infected rhesus macaques (Brenchley et al., 2004; Li et al., 2005). In 14–28 days following infection, the population of extra-lymphoid CCR5$^+$ T_{EM} was depleted up to 90% (Centlivre et al., 2007; Mattapallil et al., 2005; Okoye et al., 2007). At

* Corresponding author. Fax: +81 75 751 4812.
E-mail address: ykoyanag@virus.kyoto-u.ac.jp (Y. Koyanagi).
[1] These authors contributed equally to this study.

0042-6822/$ – see front matter © 2009 Elsevier Inc. All rights reserved.
doi:10.1016/j.virol.2009.08.011

the same time, an obvious reduction in $CD4^+$ T lymphocytes was not found in the PB. In an attempt to compensate for the loss of $CCR5^+$ T_{EM}, $CCR5^-$ T_{CM} was persistently activated and divided in order to prevent the collapse of the T_{EM} compartment (Brenchley, Price, and Douek, 2006). However, $CCR5^-$ T_{CM} lose their regenerative capability after prolonged period of proliferation, leading to decrease in both T_{CM} and T_{EM} compartments (Brenchley, Price, and Douek, 2006). This continuous shortage in $CCR5^+$ T_{EM} and accompanying $CCR5^-$ T_{CM} exhaustion are thought to play an important role in the progression to AIDS (Centlivre et al., 2007). Although the overloading of $CD4^+$ memory T lymphocyte homeostasis serves a compelling model of immunodeficiency in SIV infection, its relevance in HIV-1 infection is still poorly defined. Therefore, it is necessary that memory T lymphocyte infection is studied in an experimental animal model reconstituted with competent human immune cells.

To investigate the dynamics of $CD4^+$ T lymphocyte depletion following HIV-1 infection and the status of HIV-1-producing cells *in vivo*, we infected human $CD34^+$ cells-transplanted newborn NOG mice (NOG-hCD34 mice) with HIV-$1_{JR\text{-}CSF}$ (R5 HIV-1) or HIV-$1_{NL4\text{-}3}$ (X4 HIV-1). Our findings indicate that X4 HIV-1 infection can cause the depletion of $CD4^+$ thymocytes which results in the reduction in both naïve and memory T lymphocytes, while R5 HIV-1 infection can selectively deplete memory $CD4^+$ T lymphocytes. Further analyses indicate that R5 HIV-1 preferentially infects $CCR7^-$ T_{EM} and that the infected cells are predominantly activated and in an actively proliferating state. These results suggest that preferential infection in the activated T_{EM} leads to selective depletion of memory $CD4^+$ T lymphocytes in R5 HIV-1-infected patients.

Results

Kinetics of PB $CD4^+$ T lymphocyte depletion in R5 and X4 HIV-1-infected mice

NOG-hCD34 mice were generated by human $CD34^+$ hematopoietic stem cell transplantation into neonatal NOG mice as described previously (Baenziger et al., 2006; Traggiai et al., 2004). A significant level of human leukocytes was maintained in the whole PB of 13–44

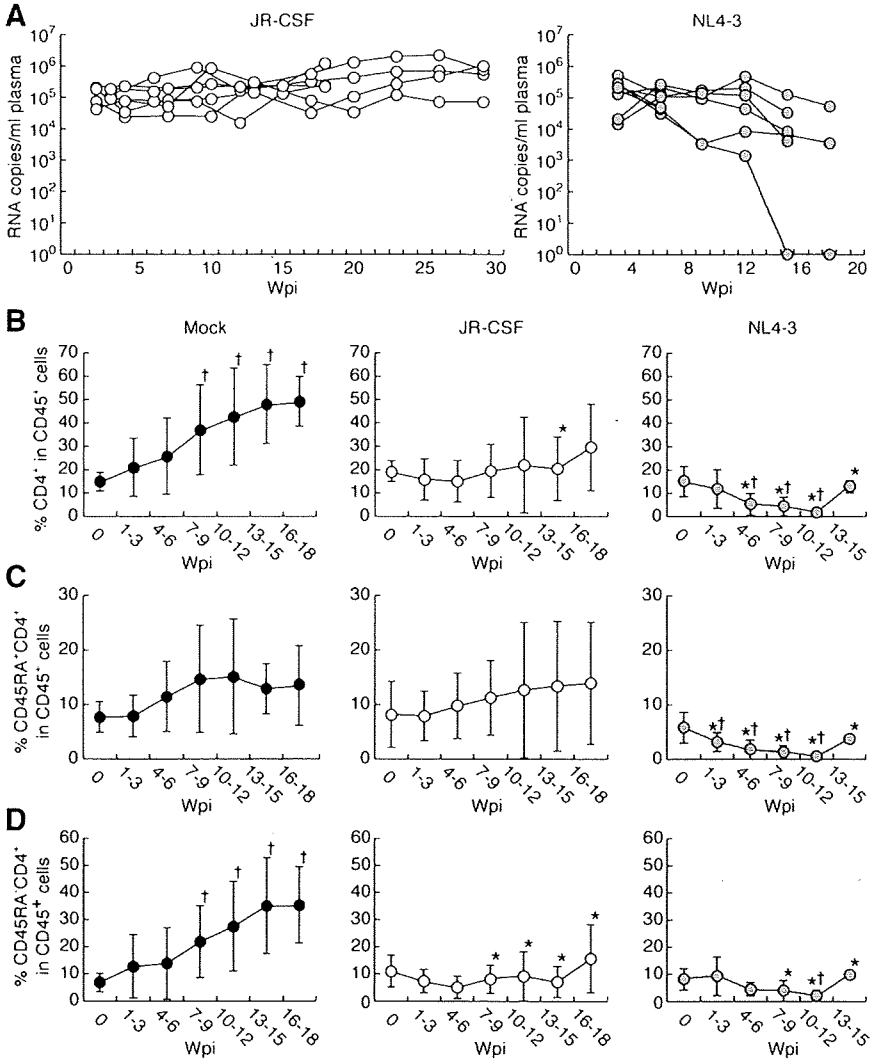

Fig. 1. Longitudinal analysis on plasma viral load and $CD4^+$ T lymphocytes in the PB of R5 and X4 HIV-1-infected mice. NOG-hCD34 mice were intraperitoneally injected with 1×10^5 $TCID_{50}$ of HIV-$1_{JR\text{-}CSF}$ ($n=7$) or HIV-$1_{NL4\text{-}3}$ ($n=8$) between 12 and 13 weeks olds. (A) The longitudinal analysis on the plasma viral load of HIV-$1_{JR\text{-}CSF}$-infected (left) and HIV-$1_{NL4\text{-}3}$-infected (right) mice. (B–D) PB was routinely sampled and analyzed for CD45RA expression in $CD4^+$ T lymphocytes from mock-infected ($n=8$), HIV-$1_{JR\text{-}CSF}$-infected ($n=7$), and HIV-$1_{NL4\text{-}3}$-infected ($n=8$) mice. We assigned data into 7 periodic groups (data taken at 0, between 1–3, 4–6, 7–9, 10–12, 13–15, and 16–18 wpi), and the average percentage and standard deviation were calculated using data obtained from each mouse during each time period. The percentages of $CD4^+$ (B), $CD45RA^+CD4^+$ (C), and $CD45RA^-CD4^+$ (D) T lymphocytes in the peripheral $CD45^+$ cells are shown. Error bars show standard deviations. Daggers represent statistical difference ($P<0.05$) when compared to the value at 0 wpi, and asterisks represent statistical difference when compared to the value obtained from the mock-infected mice.

week old mice (Supplemental Fig. 1A). Hematopoietic and lymphoid organs such as thymus, bone marrow, spleen and lymph nodes were highly repopulated with human mononuclear cells (Supplemental Figs. 1B–E). The expression of CCR5 was mainly restricted within the CD45RA$^-$ memory subset in CD4$^+$ T lymphocytes, and CXCR4 was broadly expressed on both naïve and memory T lymphocytes (Fig. 4C and data not shown) as observed in humans (Ebert and McColl, 2001).

NOG-hCD34 mice were inoculated with either an R5 HIV-1 (HIV-$1_{JR\text{-}CSF}$) or an X4 HIV-1 (HIV-$1_{NL4\text{-}3}$) between 12 and 13 weeks old. HIV-1 RNA was detected in the plasma of these mice as early as 3 weeks post-infection (wpi) and was maintained at high levels (1×10^4 to 10^6 copies per milliliter) until 28 wpi or until sacrificed (Fig. 1A). PB of these mice was then analyzed for longitudinal changes in CD4$^+$ T lymphocytes by flow cytometry. In the PB of both HIV-$1_{JR\text{-}CSF}$-infected and HIV-$1_{NL4\text{-}3}$-infected mice, depletion of human CD4$^+$ T lymphocytes was consistently found (Fig. 1B). In HIV-$1_{NL4\text{-}3}$-infected mice, both CD4$^+$CD45RA$^+$ naïve and CD4$^+$CD45RA$^-$ memory T lymphocytes were depleted, whereas in HIV-$1_{JR\text{-}CSF}$-infected mice, CD4$^+$CD45RA$^-$ memory T lymphocytes were specifically depleted (Figs. 1C and D). These data indicate that the infection with HIV-$1_{NL4\text{-}3}$ caused faster and more severe depletion of both naïve and memory subsets of CD4$^+$ T lymphocytes and the infection with HIV-$1_{JR\text{-}CSF}$ preferentially depleted memory CD4$^+$ T lymphocytes.

Thymopathy in X4 HIV-1-infected mice

To investigate the effect of HIV-1 infection on the thymopoiesis in NOG-hCD34 mice, the thymocytes from HIV-1-infected and mock-infected mice were isolated and were analyzed with flow cytometry. In mock-infected and HIV-$1_{JR\text{-}CSF}$-infected mice, CD4 and CD8 double positive (DP) thymocytes were predominant (Fig. 2A). CD4 single positive (SP) and CD8 SP thymocytes together made up a major fraction of the thymocyte population, and double negative (DN) thymocytes were only a minor fraction. In contrast, thymi from HIV-$1_{NL4\text{-}3}$-infected mice were severely depleted of both CD4 SP thymocytes and DP thymocytes (Figs. 2A–C). Furthermore, thymi from HIV-$1_{NL4\text{-}3}$-infected mice had greatly reduced number of all subsets of thymocytes (Fig. 2D). CD4 SP and DP thymocytes showed the greatest (approximately 100-fold) reduction, while CD8 SP thymocytes showed relatively milder (approximately 10-fold) reduction (Fig. 2D). These data indicate that infection with HIV-$1_{NL4\text{-}3}$ led to disturbed thymopoiesis and that HIV-$1_{JR\text{-}CSF}$ infection did not affect thymopoiesis.

Histological detection of p24-positive cells

HIV-1 p24-positive cells productively produce HIV-1 virions. Since human CD45$^+$ mononuclear cells were very few or absent in HIV-$1_{NL4\text{-}3}$-infected mice when sacrificed, they were not further analyzed (data not shown). As presented in Fig. 3, the immunohistological staining showed the presence of HIV-1 p24-positive cells in all of the bone marrow, spleen, and lymph nodes. HIV-1 p24 staining co-localized with CD4 staining. Also, a larger percentage of cells seemed to be productively infected with HIV-1 in the spleen and lymph nodes.

Depletion of splenic memory CD4$^+$ T lymphocytes

We isolated mononuclear cells from the spleen of HIV-$1_{JR\text{-}CSF}$-infected and mock-infected mice and then analyzed them by flow cytometry. As shown in Fig. 4A, the percentage of CD4$^+$ T lymphocytes in the spleen of HIV-$1_{JR\text{-}CSF}$ mice was smaller than that of mock-infected mice by 2.7-fold ($P=0.003$), showing that HIV-$1_{JR\text{-}CSF}$-infected mice had significantly fewer splenic CD4$^+$ T lymphocytes. Moreover, the percentage of splenic CD4$^+$CD45RA$^-$ memory T lymphocytes in HIV-$1_{JR\text{-}CSF}$-infected mice was smaller than that in the mock-infected mice ($P=0.007$), whereas the percentages of splenic CD4$^+$CD45RA$^+$ naive T lymphocytes were indifferent ($P=0.17$) (Fig. 4B). In mock-infected mice, a significant fraction of CD4$^+$CD45RA$^-$ T lymphocytes were CCR5$^+$ memory T lymphocytes (Fig. 4C). In contrast, in HIV-$1_{JR\text{-}CSF}$-infected mice, we found approximately 20-fold reduction in the percentage (Fig. 4C) and 100-fold reduction in the number of CD4$^+$CD45RA$^-$CCR5$^+$ memory T lymphocytes (data not shown). These results suggest that the CCR5-expressing memory CD4$^+$ T lymphocytes are depleted by direct R5 HIV-1 infection and that such reduction of CCR5-expressing CD4$^+$ T lymphocytes would lead to the decrease in whole memory CD4$^+$ T lymphocytes.

Preferential HIV-1 productive infection in CD4-negative effector memory T lymphocytes

To characterize the immunophenotypes of HIV-1 productively infected cells in NOG-hCD34 mice, splenic mononuclear cells from

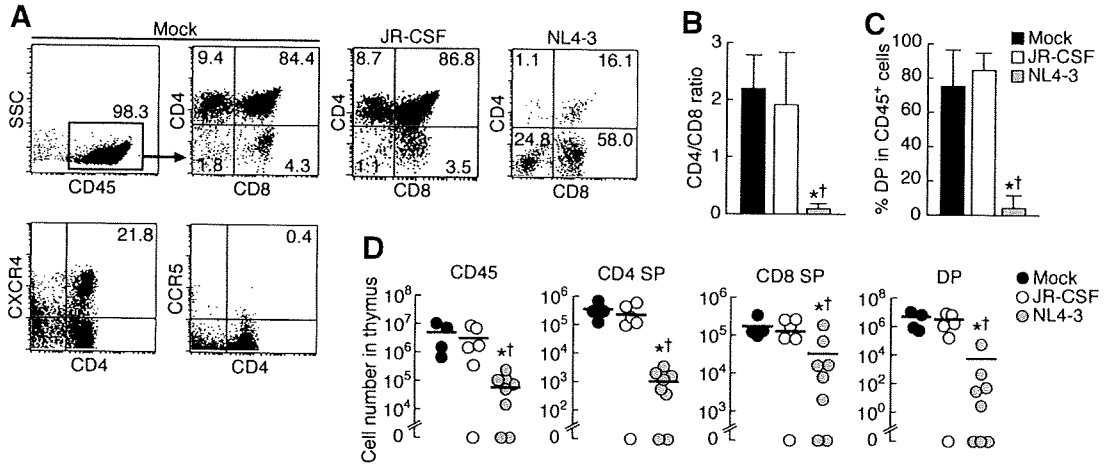

Fig. 2. Thymopathy in X4 HIV-1-infected mice. (A) Representative profile of flow cytometric analysis in thymi of mock-, HIV-$1_{JR\text{-}CSF}$-, and HIV-$1_{NL4\text{-}3}$-infected mice. The numbers in dot plots indicate the percentage of cells in CD45$^+$ thymocytes. (B and C) CD4/CD8 ratio (B) and the percentages of DP cells in CD45$^+$ thymocytes (C) in mock-infected ($n=4$), HIV-$1_{JR\text{-}CSF}$-infected ($n=5$), and HIV-$1_{NL4\text{-}3}$-infected ($n=6$) mice. (D) Number of CD45$^+$, CD4 SP, CD8 SP, and DP cells in thymi of mock-infected ($n=4$), HIV-$1_{JR\text{-}CSF}$-infected ($n=6$), and HIV-$1_{NL4\text{-}3}$-infected ($n=8$) mice. The horizontal bars in D show the average values, and the error bars in B and C show standard deviations. Asterisks indicate statistical significance ($P<0.05$) when compared to mock-infected mice, and daggers indicate statistical significance when compared to HIV-$1_{JR\text{-}CSF}$-infected mice.

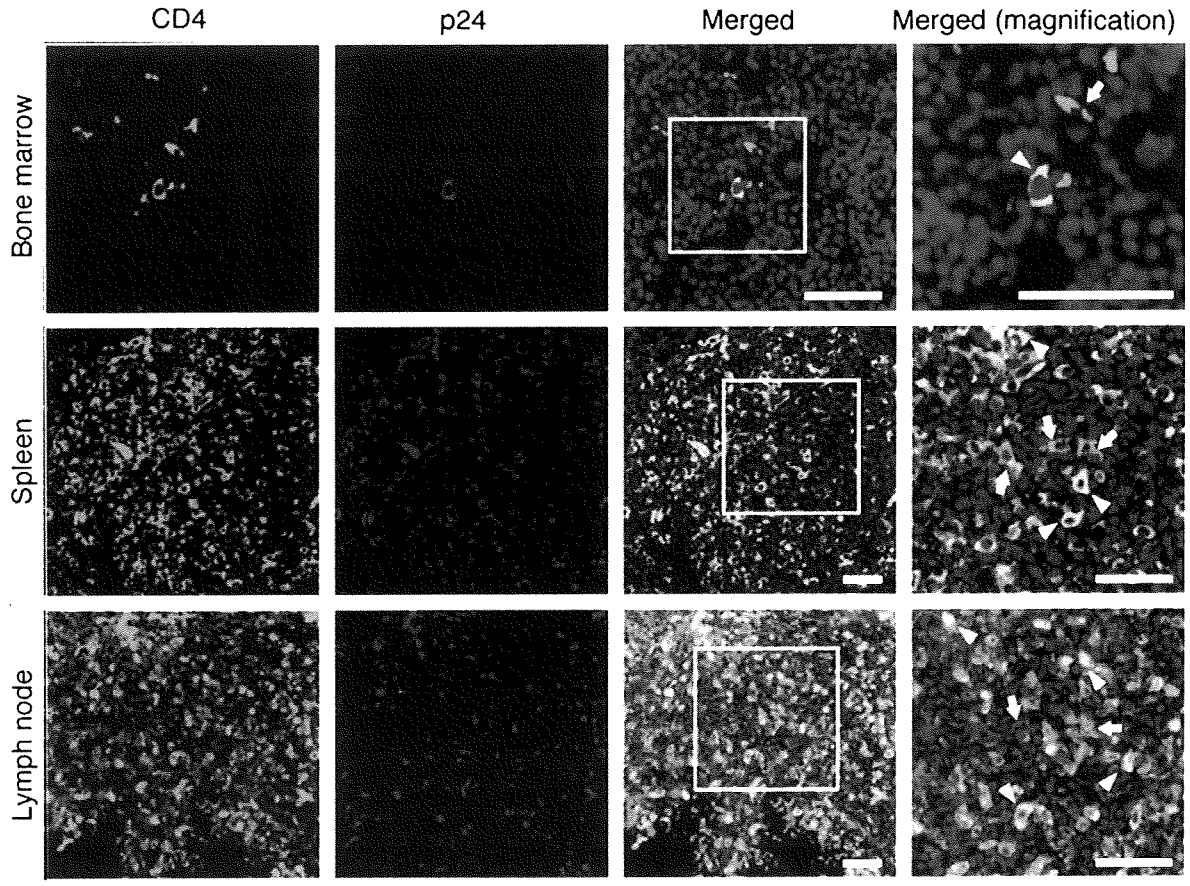

Fig. 3. Histological analysis on R5 HIV-1-infected mice. Representative immunohistological analysis of CD4 (green) and HIV-1 p24 (red) in the slices of bone marrow, spleen, and lymph nodes of HIV-$1_{JR\text{-}CSF}$-infected NOG-hCD34 mice. The low magnification images of the bone marrow slices were taken at × 80, and the high magnification images were taken at × 160. The low magnification images of the spleen and lymph nodes slices were taken at × 40, and the high magnification images were taken at × 80. The areas enclosed with the white squares were enlarged. The arrows point at representative $CD4^+$ cells and the arrowheads point at representative $CD4^+p24^+$ cells. Scale bars, 50 μm.

HIV-$1_{JR\text{-}CSF}$-infected mice were further analyzed for HIV-1 antigen p24 and the expression of lymphocyte surface markers. The anti-p24 antibody that we used did not react with any of the cells isolated from the mock-infected mice (Fig. 5A), as reported previously (Okuma et al., 2008). A significant fraction of splenic leukocytes expressed HIV-1 p24 and thus was productively infected with HIV-1 (Fig. 5A). The productively infected cells expressed surface CD3 but lacked surface CD4 (Figs. 5B and C). On average, over 90% of the $p24^+$ cells were $CD3^+$, yet only about 5% of these cells expressed surface CD4 (Fig. 5C). Also, p24-expressing cells were positive for CD45RO but not for CD45RA, suggesting that they were memory T lymphocytes ($73.7 \pm 24.3\%$ for $CD45RO^+CD45RA^-$ in $p24^+$ cells; Figs. 5D and E). Central memory T lymphocyte (T_{CM}) can be defined as a memory T lymphocyte that expresses CCR7, and effector memory T lymphocyte (T_{EM}) can be defined as a memory T lymphocyte that lacks CCR7 (Sallusto, Geginat, and Lanzavecchia, 2004). In p24-positive cells, $88.0 \pm 3.75\%$ was negative for CCR7 (Figs. 5D and F), suggesting that T_{EM} dominantly and productively infect with HIV-1.

Productive HIV-1 infection in activated and dividing lymphocytes

To investigate the activation status of the productively infected cells, splenic mononuclear cells were stained with anti-p24, anti-Ki67, and anti-CD69 antibodies. Ki67 antigen is exclusively expressed in proliferating cells, and CD69 is expressed on the surface of the activated cells at the early phase (Sereti et al., 2007; Vatakis et al., 2007). In splenic $CD4^+$ T lymphocytes from mock-infected mice or p24-negative splenocytes from HIV-$1_{JR\text{-}CSF}$-infected mice, only a minor fraction of the cells expressed either Ki67 or CD69 (Figs. 6A and B). In contrast, the majority of p24-positive splenocytes from HIV-$1_{JR\text{-}CSF}$-infected mice expressed Ki67 and/or CD69 (Figs. 6A and B). Also, the percentage of cells positive for both Ki67 and CD69 were higher in p24-positive cells than in p24-negative splenocytes from HIV-$1_{JR\text{-}CSF}$-infected mice and in splenic $CD4^+$ T lymphocytes from mock-infected mice (Fig. 6B). These results indicate that a significantly higher frequency of p24-positive cells is activated and/or proliferating cells. Notably, although the frequency was significantly low, we could detect $Ki67^-CD69^-$ resting T lymphocytes in p24-positive cells (Figs. 6A and B).

To further analyze the cell cycle of HIV-1 productively infected cells (i.e., p24-positive cells), we carried out Hoechst staining, which quantifies DNA content of the cells. Ki67 staining in combination with the Hoechst staining will sort cells into those in G_0/G_{1a}, G_{1b}, and $S/G_2/M$ phases of the cell cycle (Wilpshaar et al., 2000). As shown in Fig. 6C, non-stimulated human peripheral blood leukocytes (PBLs) predominantly exist in G_0/G_{1a} phases ($Ki67^-Hoechst^{low}$, lower left in the quadrant), while PHA-activated human PBLs predominantly exist in cycling G_{1b} phase ($Ki67^+Hoechst^{low}$, upper left in the quadrant) and $S/G_2/M$ phases ($Ki67^+Hoechst^{high}$, upper right in the quadrant). By using this method, we observed that p24-positive cells contained a significantly higher frequency of cells in the G_{1b} phase. In addition, the percentage of p24-positive cells in $S/G_2/M$ phases was significantly higher than $CD4^+$ splenocytes from mock-infected mice (Figs. 6D and E). These findings indicate that the majority of HIV-1-producing cells in the spleen of R5 HIV-1-infected mice are activated and in cycling phase. On the other hand, we detected the p24-

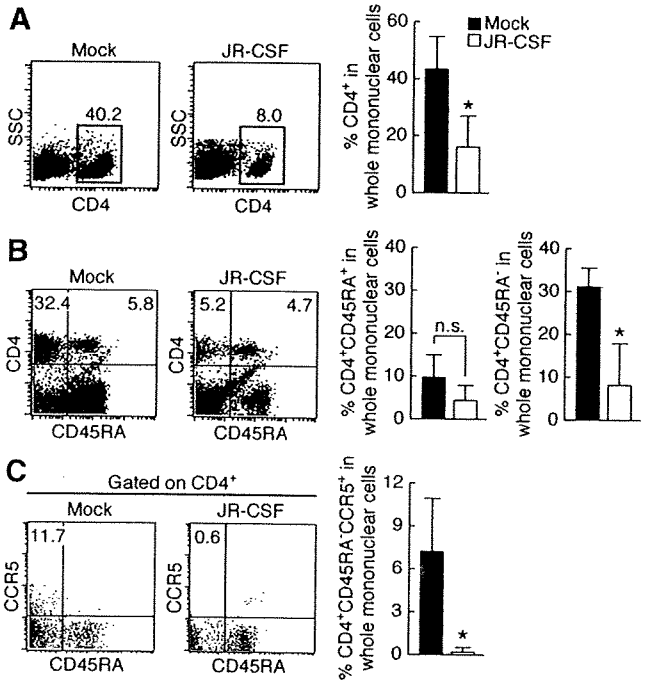

Fig. 4. The effect of R5 HIV-1 infection on the splenic $CD4^+$ T lymphocyte population. (A–C) Staining of splenic nucleated cells from the spleen of mock-infected ($n=4$) and HIV-$1_{JR\text{-}CSF}$-infected ($n=4$) mice were stained with CD4 (A), CD4 and CD45RA (B), and CCR5, CD4, and CD45RA (C). Representative profiles are shown, and the numbers in dot plots indicate the percentage of cells in $CD45^+$ splenic human leukocytes (A and B) or in $CD4^+$ cells (C). The graphs show the percentages of cells possessing each phenotype in whole mononuclear cells. The error bars show standard deviations. Asterisks indicate statistical significance ($P<0.05$) when compared to mock-infected mice.

positive splenocytes in G_0/G_{1a} phases, although the frequency was significantly lower than p24-negative splenocytes or $CD4^+$ splenocytes from mock-infected mice (Figs. 6D and E). These data suggest that a fraction of resting cells productively infects HIV-1. Moreover, we detected the significantly higher percentage of cells in $S/G_2/M$ phases in splenic p24-negative cells of HIV-$1_{JR\text{-}CSF}$-infected mice when comparing to that in splenic $CD4^+$ T lymphocytes of mock-infected mice (Figs. 6D and E).

Discussion

To investigate the mechanisms of $CD4^+$ T lymphocyte depletion by HIV-1 infection, we utilize human $CD34^+$ cells-transplanted NOG mice (Ito et al., 2002) and demonstrate that human $CD4^+$ T lymphocytes were differentially affected by X4 and R5 HIV-1 infection (Figs. 1–4). X4 virus induced immediate depletion of both naïve and memory $CD4^+$ T lymphocytes in periphery, while R5 virus gradually depleted memory $CD4^+$ T lymphocytes in the PB (Fig. 1) and spleen (Fig. 4). Our data suggest that distinctive pathogenesis of X4 and R5 viruses in NOG-hCD34 mice was caused by thymopathy (Fig. 2) and preferential infection of activated and dividing T_{EM} (Figs. 5 and 6), respectively. This is the first report addressing the mechanisms and dynamics of HIV-1-induced $CD4^+$ T lymphocyte depletion *in vivo*.

As previously shown in X4 SHIV-infected macaques (Ho et al., 2005; Nishimura et al., 2004), we observed the drastic loss of both naïve and memory T lymphocytes by X4 HIV-1-infected NOG-hCD34 mice (Fig. 1). We also found that $CD4^+$ thymocytes in NOG-hCD34 mice abundantly express CXCR4 (Fig. 2A) and that the $CD4^+$ thymocytes including DP and CD4 SP were preferentially reduced in HIV-$1_{NL4\text{-}3}$-infected mice (Fig. 2). It has been reported that intrathymic infection by X4 HIV-1 can lead to severe T lymphocytopenia (Berkowitz et al., 1998; Schnittman et al., 1990; Ye, Kirschner, and Kourtis, 2004). Therefore, our results suggest that the primary mechanism for naïve and memory T lymphocyte depletion in X4 virus infection can be attributed to impaired thymopoiesis caused by intrathymic infection.

In contrast to X4 HIV-1 infection, the depletion of PB $CD4^+$ T lymphocytes was more gradual and less intense in R5 HIV-1 infection and was confined to $CD45RA^-$ memory $CD4^+$ T lymphocytes (Fig. 1D). The selective depletion of memory $CD4^+$ T lymphocytes by R5 infection was also found in the spleen (Fig. 4). On the other hand, thymopathy was not detected in HIV-$1_{JR\text{-}CSF}$-infected mice (Fig. 2). These findings suggest that the selective depletion of memory $CD4^+$ T lymphocytes in PB and spleen of HIV-$1_{JR\text{-}CSF}$-infected mice caused through a different mechanism from HIV-$1_{NL4\text{-}3}$, and the mechanisms are further discussed below.

To investigate the mechanisms of memory $CD4^+$ T lymphocyte depletion in R5 HIV-1 infection in-depth, a series of flow cytometric analyses was carried out. The majority of $p24^+$ productively infected cells in the spleen were $CD3^+$ T lymphocytes (Figs. 5B and C). However, these infected cells were negative for surface CD4 (Figs. 5B

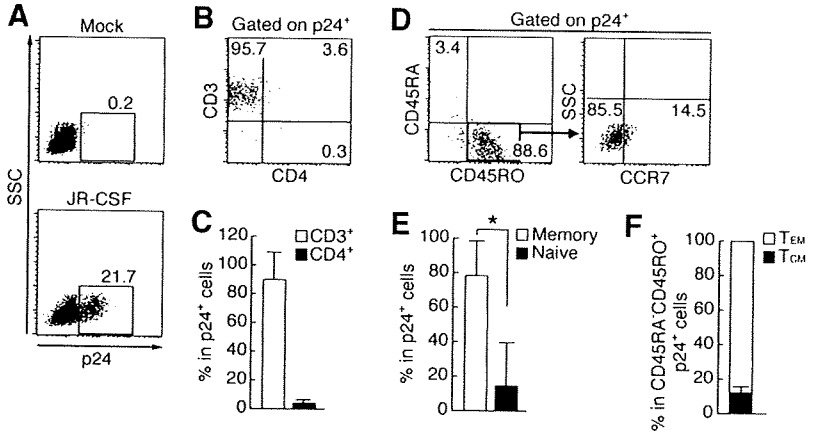

Fig. 5. Phenotype of productively infected $p24^+$ cells in the spleen of R5 HIV-1-infected mice. (A) Representative profiles of flow cytometric p24 staining in splenic nucleated cells of mock-infected ($n=4$) and HIV-$1_{JR\text{-}CSF}$-infected ($n=6$) mice. The numbers indicate the percentage of cells in splenic nucleated cells. (B and C) Staining of splenic nucleated cells of HIV-$1_{JR\text{-}CSF}$-infected mice for p24, CD3, and CD4. Representative profiles are shown in B, and the numbers in each quadrant indicate the percentage of cells in $p24^+$ cells. The percentages of each population in $p24^+$ cells are shown in C. (D–F) Staining of splenic nucleated cells of HIV-$1_{JR\text{-}CSF}$-infected mice for p24, CD45RA, CD45RO, and CCR7. Representative profiles are shown in D, and the numbers in each quadrant indicate the percentage of cells in $p24^+$ cells (left) or in $p24^+CD45RA^-CD45RO^+$ cells (right). The percentages of memory ($CD45RA^-CD45RO^+$) and naïve ($CD45RA^+CD45RO^-$) phenotyped cells in $p24^+$ cells are shown in E. The percentages of T_{EM} ($CCR7^-CD45RA^-CD45RO^+$) and T_{CM} ($CCR7^+CD45RA^-CD45RO^+$) in $p24^+$ cells are shown in F. The error bars in C, E, and F show standard deviations. Asterisks indicate statistical significance ($P<0.05$).

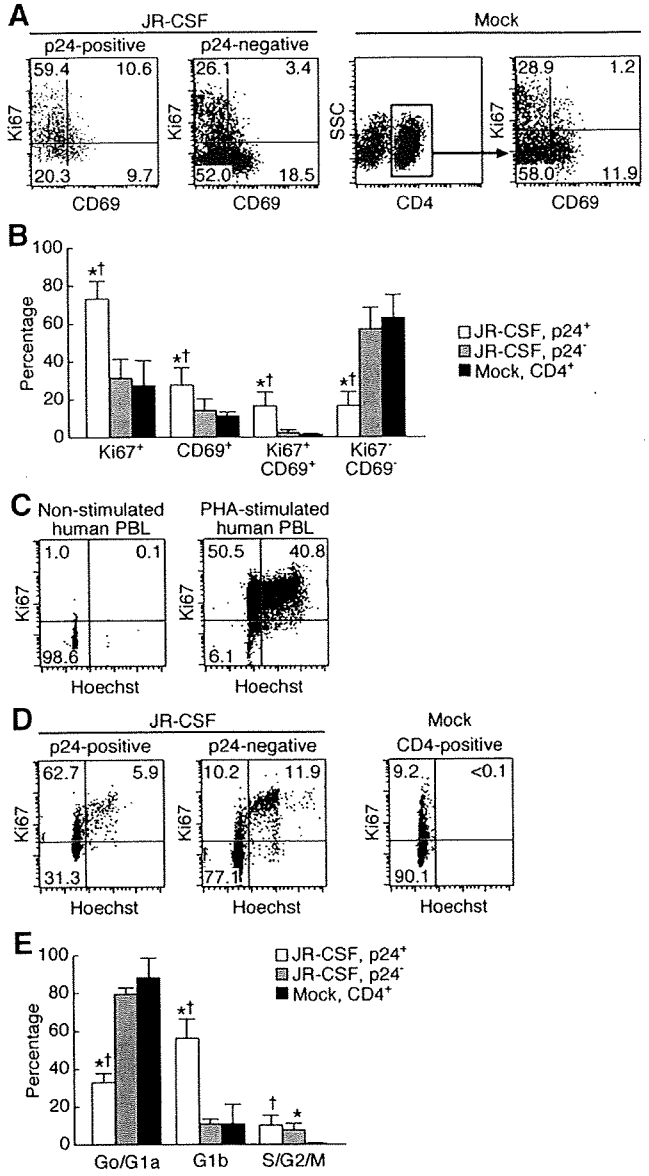

Fig. 6. Cell cycle analyses on productively infected $p24^+$ cells in the spleen of R5 HIV-1-infected mice. (A and B) Staining of splenic nucleated cells of mock-infected ($n=3$) and HIV-$1_{JR\text{-}CSF}$-infected ($n=4$) mice for Ki67, CD69, and either CD4 or p24. Representative profiles are shown in A, and each number indicates the percentage of cells in each quadrant. The graph in B shows the average percentages of cells possessing each population. (C) A representative profile of cell cycle analysis on non-stimulated human PBL (left panel) and PHA-activated human PBL (right panel) by using anti-Ki67 antibody and Hoechst. Each number indicates the percentage of cells in each quadrant. $Ki67^-Hoechst^{low}$ (lower left in quadrant) indicates G_0/G_{1a} phase, while $Ki67^+Hoechst^{low}$ (upper left in quadrant) and $Ki67^+Hoechst^{high}$ (upper right in quadrant) indicate G_{1b} and $S/G_2/M$ phases, respectively. (D and E) Staining of splenic nucleated cells of mock-infected mice ($n=4$) for CD4, Ki67, and Hoechst, and HIV-$1_{JR\text{-}CSF}$-infected mice ($n=4$) for p24, Ki67, and Hoechst. Representative profiles are shown in D, and each number indicates the percentage of cells in each quadrant. The graph in E shows the average percentages of cells in each population. The error bars in B and E show standard deviations. Asterisks indicate statistical significance ($P<0.05$) when compared to the value of p24-negative cells in HIV-$1_{JR\text{-}CSF}$-infected mice, and daggers indicate statistical significance when compared to the value of CD4-positive cells in mock-infected mice.

and C), although immunohistological analysis revealed that splenic $p24^+$ cells expressed CD4 molecules (Fig. 3). These results suggest that surface CD4 molecules are severely down-regulated following infection. In fact, it has been well documented that HIV-1 gene products such as *Nef* (Fackler, Alcover, and Schwartz, 2007; Roeth and Collins, 2006), *Env* (Crise, Buonocore, and Rose, 1990), and *Vpu* (Bour and Strebel, 2003; Geleziunas, Bour, and Wainberg, 1994) have the potential to down-regulate CD4 molecules from the surface of infected cells (Lindwasser, Chaudhuri, and Bonifacino, 2007). Similar down-regulation of surface CD4 has also been reported in lymph nodes and PB of HIV-1-infected patients (Cheney et al., 2006; Kaiser et al., 2007; Marodon et al., 1999). Therefore, this down-regulation of surface CD4 molecules in HIV-$1_{JR\text{-}CSF}$-infected mice is physiologically relevant and can play a role in the reduction of $CD4^+$ T lymphocytes.

In HIV-$1_{JR\text{-}CSF}$-infected mice, more than 80% of the productively infected cells were activated and in cycling phase (Fig. 6). It has been well known that activated cells massively produce HIV-1 virions (Ho et al., 1995). Therefore, this result suggests that the persistent viremia in R5 infection (Fig. 1A) is primarily due to the productive infection in the activated and proliferating cells. On the other hand, a fraction of infected cells were quiescent T lymphocytes negative for both activation and proliferation markers (Fig. 6). It is thought that HIV-1 cannot manifest productive infection in quiescent cells (Stevenson et al., 1990; Zack et al., 1990). However, studies on *ex vivo* infected human tonsil histocultures (Eckstein et al., 2001; Kinter et al., 2003), small intestines and cervix of SIV-infected rhesus macaques (Li et al., 2005; Zhang et al., 1999; Zhang et al., 2004), and HIV-1-infected patients (Zhang et al., 1999) have established that quiescent T lymphocytes residing in the lymphoid tissues are capable of supporting productive SIV or HIV-1 infection. Our results provide further support that productive infection of HIV-1 can take place in non-dividing cells, presumably resting T lymphocytes, in NOG-hCD34 mice. Productive infection not only in proliferative cells but also in quiescent cells may be an important factor in $CD4^+$ T lymphocyte depletion and persistent virus infection.

The preferential infection of $CD45RO^+CD45RA^-$ memory T lymphocytes with R5 HIV-1 is also the evidence supportive for the selective depletion of memory $CD4^+$ T lymphocytes (Figs. 5D and E). Nevertheless, only $16.3\pm9.7\%$ of splenic $CD4^+$ T lymphocytes expressed CCR5 in NOG-hCD34 mice, and the severe depletion of memory T lymphocytes in R5 HIV-1 infection cannot be explained by cell death caused by infection solely. In this regard, it has been reported that memory $CD4^+$ T lymphocyte reduction in SIV-infected macaques can be initiated by specific disruption of T_{EM} due to its preferential infection in the acute phase (Centlivre et al., 2007; Mattapallil et al., 2005; Okoye et al., 2007). In response to the T_{EM} reduction, T_{CM} proliferates and supplies *de novo* T_{EM} (Sallusto, Geginat, and Lanzavecchia, 2004). However, Brenchley et al. (2004) and Okoye et al. (2007) have reported that R5 virus infection induces chronic immune activation in macaques, which leads to the attenuation of regenerative capacity of T_{CM} (Brenchley et al., 2004; Okoye et al., 2007). In addition to the depletion of T_{EM} by direct infection, the attenuation of regenerative potential of T_{CM} causes not only the loss of T_{CM} but also the shortage of T_{EM} and eventually leads to the reduction of whole memory T lymphocytes (Brenchley et al., 2004; Okoye et al., 2007). This hypothesis of the dynamics of $CD4^+$ T lymphocyte depletion has been helpful for explaining the memory $CD4^+$ T lymphocyte in effector sites of SIV-infected macaques. Our observations in HIV-$1_{JR\text{-}CSF}$-infected mice, the severe depletion of memory T lymphocytes despite the limited availability of CCR5-expressing $CD4^+$ T lymphocytes and the preferential infection in T_{EM}, can be explained by the aforementioned hypothesis proposed in the previous literature (Brenchley et al., 2004; Okoye et al., 2007). Notably, we found that the frequency of cells in $S/G_2/M$ phases elevated in splenic p24-negative cells of HIV-$1_{JR\text{-}CSF}$-infected mice when comparing to that in splenic $CD4^+$ T lymphocytes of mock-infected mice (Figs. 6D and E). These data may explain that HIV-1 pathophysiology is caused by accelerated cells division, ultimately leading to the exhaustion of $CD4^+$ T lymphocytes. Taken together, our findings suggest that the selective infection of T_{EM} may be an important event that governs $CD4^+$ T lymphocyte depletion not

only in the effector sites of macaques during SIV infection but also in lymphoid organs during HIV-1 infection.

In summary, we showed differential $CD4^+$ T lymphocyte reduction in R5 and X4 HIV-1 infection. We report for the first time the selective depletion of memory $CD4^+$ T lymphocytes and the preferential infection of T_{EM} in an experimental model of R5 HIV-1 infection. Our data suggest that HIV-1 infection in T_{EM} can be an important step leading to $CD4^+$ T lymphocyte decline. Our findings confirm the applicability of NOG-hCD34 mice as a useful model to study the dynamics of HIV-1 pathogenesis including $CD4^+$ T lymphocytes depletion *in vivo*.

Materials and methods

Mice

NOD/SCID/IL-2Rγ^{null} (NOG) mice (Ito et al., 2002) were obtained from the Central Institute for Experimental Animals (Kanagawa, Japan). The mice were maintained under specific pathogen-free conditions and were handled in accordance with the Regulation on Animal Experimentation at Kyoto University.

Purification and transplantation of cord blood-derived CD34 cells

The purification of cord blood-derived CD34 cells was conducted as described previously (Ishikawa et al., 2005; Ito et al., 2002). Fresh human cord blood was obtained with parent written informed consent from healthy full-term newborns and CD34 MicroBead Kit (Miltenyi Biotec Inc, Auburn, CA) was used to isolate $hCD34^+$ cells according to the manufacturer's instructions. Cells were either stored at −80 °C or immediately transplanted when newborn mice were available. $CD34^+$ cells ($5–12\times10^4$) were intrahepatically injected into newborn mice of ages between 0 and 2 days after total radiation of 10 cGy per mouse in MBR-1520 x-ray irradiator (Hitachi Medico, Tokyo, Japan).

Peripheral blood collection and isolation of nucleated cells from organs

PB was routinely taken from NOG-hCD34 mice under ether anesthesia via retro-orbital venousplexus as described previously (Ishikawa et al., 2005). The red blood cells in the PB were lysed in preparation for flow cytometric analysis in 1× BD lysis buffer (BD Pharmingen, San Diego, CA). When the mice were sacrificed, PB was taken by cardiac puncture. Lymph nodes, thymi, spleen, and bone marrow were taken from HIV-1-infected and mock-infected mice upon sacrifice for histological or flow cytometric analysis. Lymph nodes and thymi were gently homogenized using a homogenizer pestle and spleens were crushed and rubbed on a steal mesh with 1-mm grids to generate single cell suspensions in RPMI 1640 supplemented with 4% fetal calf serum (FCS). To collect bone marrow, thigh bones were dissected at both ends and the interior was flushed with RPMI 1640 supplemented with 4% FCS. The cells were immediately used for flow cytometric analysis or stored in Cell Banker (Juji Field Inc., Tokyo, Japan) at −80 °C until use. As there are some variations in the combination of antibodies used to study the human cell population in each mouse, the number of data collected for each surface marker may differ. Data used for any longitudinal analysis were taken from identical mice.

Flow cytometric analysis of human blood cells in transplanted mice

The staining for flow cytometric analysis was done with some modifications to the protocol previously described (Sato et al., 2008). Briefly, for the surface staining, the cells were blocked with FcR blocker (Miltenyi Biotec Inc) for 5 min at room temperature (RT) and then incubated with the appropriate antibodies at optimum concentration in 1× phosphate-buffered saline (PBS) containing 2% FCS for 30 min at 4 °C. Fluorescein isothiocyanate-conjugated (FITC-conjugated) anti-human CD19 (HD37; Dako, Tokyo, Japan), CD8 (DK25; Dako), CD14 (TUK4; Miltenyi Biotec Inc), CD4 (L3T4; eBioscience, San Diego, CA), CD3 (UCHT1; BD Pharmingen, San Diego, CA), CCR5 (3A9; BD Pharmingen), and CD303/BDCA2 (AC144; Miltenyi Biotec Inc) mouse IgG monoclonal antibodies (mAb); phycoerythrin-conjugated anti-human CD3 (UCHT1; Dako), CD4 (MT310; Dako), CD34 (AC136; Miltenyi Biotec Inc), CD11c (B-ly6; BD Pharmingen), CXCR4 (12G5; BD Pharmingen), CCR7 (FAB197; R&D systems, Abingdon, UK), and CCR5 (3A9; BD Pharmingen) mouse IgG mAb; biotinylated anti-human CD45 (H130; eBioscience), CD45RA (HI-100; BD Pharmingen), CD8 (RPA-T8; BD Pharmingen), CD4 (RPA-T4; BD Pharmingen), and mouse IgG mAb; peridinin-chlorophyll-conjugated (PerCP-conjugated) anti-human CD69 (L78; BD Immunocytometry Systems, San Jose, CA) mouse IgG mAb; PE-Cy5-conjugated anti-human HLA-DR (G46-6; BD Pharmingen) mouse IgG mAb; allophycocyamin-conjugated anti-human CD45RO (UCHL1; BD Pharmingen) and CD8 (DK25; Dako) mouse IgG mAb were used. Each antibody was controlled with appropriate isotype antibodies purchased from Dako and BD Pharmingen. Streptavidin-PerCP (SA-PerCP) was purchased from BD Immunocytometry Systems. Following the incubation, the cells were washed and further incubated with SA-PerCP for 30 min at 4 °C, if needed. For the intracellular staining, the cells were permeabilized and fixed by treatment with BD Cytoperm/Cytofix solution (BD Pharmingen) and were stained with FITC-conjugated anti-HIV-1 p24 (clone 2C2) (Okuma et al., 2008) and anti-human Ki67 (B56; BD Pharmingen) mouse IgG mAb for 30 min at 4°C in 1× BD PermWash buffer (BD Pharmingen). For DNA staining to analyze cell cycle, the cells were incubated with Hoechst33342 (Invitrogen, Carlsbad, CA) for 30 min at 4 °C as described previously (Wilpshaar et al., 2000). Data collection was performed on BD FACSCan (BD Biosciences) for 3-color staining, BD FACSCalibur (BD Biosciences) for 4-color staining, and BD FACSCanto (BD Biosciences) for cell cycle analyses using Hoechst33342, and the obtained data were analyzed with CellQuest software (BD Immunocytometry System, San Jose, CA).

HIV-1 infection

NOG mice were injected intraperitoneally with RPMI 1640 ($n=8$) or 1×10^5 50% tissue culture infective doses ($TCID_{50}$) of $HIV\text{-}1_{JR\text{-}CSF}$ ($n=7$) or $HIV\text{-}1_{NL4\text{-}3}$ ($n=8$) between 12 and 13 weeks of ages. The viruses used were prepared by transfection as previously described (Sato et al., 2008). Infectious titers in the form of $TCID_{50}$ of each virus stock were determined by endpoint dilution with phytohemagglutinin-activated PBMCs as described (Koyanagi et al., 1997).

Detection of HIV-1 RNA in the plasma of infected mice

The detection of HIV-1 RNA in the plasma of the infected mice was routinely carried out using Amplicor HIV-1 monitor v1.5 according to the manufacturer's protocol (Roche Diagnostics, Mannheim, Germany).

Immunohistological analysis

Organs were fixed in 1× PBS containing 4% paraformalhyde and embedded in OCT compound (Sakura Finetechnical, Tokyo, Japan) after immersion in 10%–20% gradient sucrose. The OCT embedded organs were then sliced and were permeabilized with 0.1% Triton-X at RT for 10 min, incubated three times with 10 mM glycine for 5 min and blocked with 5% normal goat serum at RT for 1 hr. The sections were then incubated with mouse anti-HIV-1 p24 (Kal-1; Dako) IgG mAb at 4°C overnight, followed by incubation with Alexa Fluor 488-conjugated goat anti-mouse IgG (Invitrogen) at RT for 2 hr. The sections were further incubated with biotinylated mouse anti-

human CD4 IgG mAb (RFT-4g; Southern Biotech, Birmingham, AL) at 4°C overnight, followed by incubation with Streptavidin–Alexa Fluor 647 (Invitrogen) and Hoeschst33342 at RT for 2 hr. All the antibody staining was performed in blocking solution. Images were acquired with a Leica TCS SP2 AOBS confocal laser microscope (Leica Microsystems, Heidelberg, Germany).

Statistical analysis

Data were expressed as an average with standard deviation. Significant differences between data groups were determined by Student's *t* test or paired *t* test. A *P* value less than 0.05 was considered significantly different.

Acknowledgments

We would like to thank Peter Gee (Institute for Virus Research, Kyoto University) for proofreading of our manuscript and Munetada Haruyama (the Department of Pediatrics, Kyoto University) for their generous help in our study. We also would like to express our appreciation for Ms. Kotubu Misawa's dedicated support. This work was supported by a Grant-in-Aid for Scientific Research on Priority Areas from the Ministry of Education, Culture, Sports, Sciences, and Technology of Japan; a Health and Labour Science Research Grant (Research on Publicly Essential Drugs and Medical Devices) from the Ministry of Health, Labor and Welfare of Japan; and Japan Human Science Foundation. K.S. was supported by Research Fellowships of the Japan Society for the Promotion of Science for Young Scientists. Y. K. was supported by a grant from the Naito Foundation.

Appendix A. Supplementary data

Supplementary data associated with this article can be found, in the online version, at doi:10.1016/j.virol.2009.08.011.

References

Ambrose, Z., KewalRamani, V.N., Bieniasz, P.D., Hatziioannou, T., 2007. HIV/AIDS: in search of an animal model. Trends Biotechnol. 25, 333–337.

Baenziger, S., Tussiwand, R., Schlaepfer, E., Mazzucchelli, L., Heikenwalder, M., Kurrer, M.O., Behnke, S., Frey, J., Oxenius, A., Joller, H., Aguzzi, A., Manz, M.G., Speck, R.F., 2006. Disseminated and sustained HIV infection in $CD34^+$ cord blood cell-transplanted $Rag2^{-/-}\gamma_c^{-/-}$ mice. Proc. Natl. Acad. Sci. U. S. A. 103, 15951–15956.

Berger, E.A., Murphy, P.M., Farber, J.M., 1999. Chemokine receptors as HIV-1 coreceptors: roles in viral entry, tropism, and disease. Annu. Rev. Immunol. 17, 657–700.

Berkowitz, R.D., Alexander, S., Bare, C., Linquist-Stepps, V., Bogan, M., Moreno, M.E., Gibson, L., Wieder, E.D., Kosek, J., Stoddart, C.A., McCune, J.M., 1998. CCR5- and CXCR4-utilizing strains of human immunodeficiency virus type 1 exhibit differential tropism and pathogenesis *in vivo*. J. Virol. 72, 10108–10117.

Bour, S., Strebel, K., 2003. The HIV-1 Vpu protein: a multifunctional enhancer of viral particle release. Microbes. Infect. 5, 1029–1039.

Brenchley, J.M., Price, D.A., Douek, D.C., 2006. HIV disease: fallout from a mucosal catastrophe? Nat. Immunol. 7, 235–239.

Brenchley, J.M., Schacker, T.W., Ruff, L.E., Price, D.A., Taylor, J.H., Beilman, G.J., Nguyen, P.L., Khoruts, A., Larson, M., Haase, A.T., Douek, D.C., 2004. $CD4^+$ T cell depletion during all stages of HIV disease occurs predominantly in the gastrointestinal tract. J. Exp. Med. 200, 749–759.

Centlivre, M., Sala, M., Wain-Hobson, S., Berkhout, B., 2007. In HIV-1 pathogenesis the die is cast during primary infection. AIDS 21, 1–11.

Cheney, K.M., Kumar, R., Purins, A., Mundy, L., Ferguson, W., Shaw, D., Burrell, C.J., Li, P., 2006. HIV type 1 persistence in $CD4^-/CD8^-$ double negative T cells from patients on antiretroviral therapy. AIDS Res. Hum. Retroviruses 22, 66–75.

Crise, B., Buonocore, L., Rose, J.K., 1990. CD4 is retained in the endoplasmic reticulum by the human immunodeficiency virus type 1 glycoprotein precursor. J. Virol. 64, 5585–5593.

Ebert, L.M., McColl, S.R., 2001. Coregulation of CXC chemokine receptor and CD4 expression on T lymphocytes during allogeneic activation. J. Immunol. 166, 4870–4878.

Eckstein, D.A., Penn, M.L., Korin, Y.D., Scripture-Adams, D.D., Zack, J.A., Kreisberg, J.F., Roederer, M., Sherman, M.P., Chin, P.S., Goldsmith, M.A., 2001. HIV-1 actively replicates in naive $CD4^+$ T cells residing within human lymphoid tissues. Immunity 15, 671–682.

Fackler, O.T., Alcover, A., Schwartz, O., 2007. Modulation of the immunological synapse: a key to HIV-1 pathogenesis? Nat. Rev. Immunol. 7, 310–317.

Geleziunas, R., Bour, S., Wainberg, M.A., 1994. Cell surface down-modulation of CD4 after infection by HIV-1. FASEB J. 8, 593–600.

Ho, D.D., Neumann, A.U., Perelson, A.S., Chen, W., Leonard, J.M., Markowitz, M., 1995. Rapid turnover of plasma virions and CD4 lymphocytes in HIV-1 infection. Nature 373, 123–126.

Ho, S.H., Shek, L., Gettie, A., Blanchard, J., Cheng-Mayer, C., 2005. V3 loop-determined coreceptor preference dictates the dynamics of $CD4^+$-T-cell loss in simian–human immunodeficiency virus-infected macaques. J. Virol. 79, 12296–12303.

Ishikawa, F., Yasukawa, M., Lyons, B., Yoshida, S., Miyamoto, T., Yoshimoto, G., Watanabe, T., Akashi, K., Shultz, L.D., Harada, M., 2005. Development of functional human blood and immune systems in NOD/SCID/IL2 receptor γ $chain^{null}$ mice. Blood 106, 1565–1573.

Ito, M., Hiramatsu, H., Kobayashi, K., Suzue, K., Kawahata, M., Hioki, K., Ueyama, Y., Koyanagi, Y., Sugamura, K., Tsuji, K., Heike, T., Nakahata, T., 2002. NOD/SCID/γ_c^{null} mouse: an excellent recipient mouse model for engraftment of human cells. Blood 100, 3175–3182.

Kaiser, P., Joos, B., Niederost, B., Weber, R., Gunthard, H.F., Fischer, M., 2007. Productive human immunodeficiency virus type 1 infection in peripheral blood predominantly takes place in CD4/CD8 double-negative T lymphocytes. J. Virol. 81, 9693–9706.

Kinter, A., Moorthy, A., Jackson, R., Fauci, A.S., 2003. Productive HIV infection of resting $CD4^+$ T cells: role of lymphoid tissue microenvironment and effect of immunomodulating agents. AIDS Res. Hum. Retroviruses 19, 847–856.

Koyanagi, Y., Tanaka, Y., Ito, M., Yamamoto, N., 2008. Humanized mice for human retrovirus infection. Curr. Top Microbiol. Immunol. 324, 133–148.

Koyanagi, Y., Tanaka, Y., Kira, J., Ito, M., Hioki, K., Misawa, N., Kawano, Y., Yamasaki, K., Tanaka, R., Suzuki, Y., Ueyama, Y., Terada, E., Tanaka, T., Miyasaka, M., Kobayashi, T., Kumazawa, Y., Yamamoto, N., 1997. Primary human immunodeficiency virus type 1 viremia and central nervous system invasion in a novel hu-PBL-immunodeficient mouse strain. J. Virol. 71, 2417–2424.

Li, Q., Duan, L., Estes, J.D., Ma, Z.M., Rourke, T., Wang, Y., Reilly, C., Carlis, J., Miller, C.J., Haase, A.T., 2005. Peak SIV replication in resting memory $CD4^+$ T cells depletes gut lamina propria $CD4^+$ T cells. Nature 434, 1148–1152.

Lindwasser, O.W., Chaudhuri, R., Bonifacino, J.S., 2007. Mechanisms of CD4 downregulation by the Nef and Vpu proteins of primate immunodeficiency viruses. Curr. Mol. Med. 7, 171–184.

Lusso, P., 2006. HIV and the chemokine system: 10 years later. EMBO J. 25, 447–456.

Marodon, G., Warren, D., Filomio, M.C., Posnett, D.N., 1999. Productive infection of double-negative T cells with HIV *in vivo*. Proc. Natl. Acad. Sci. U. S. A. 96, 11958–11963.

Mattapallil, J.J., Douek, D.C., Hill, B., Nishimura, Y., Martin, M., Roederer, M., 2005. Massive infection and loss of memory $CD4^+$ T cells in multiple tissues during acute SIV infection. Nature 434, 1093–1097.

McCune, J.M., 2001. The dynamics of $CD4^+$ T-cell depletion in HIV disease. Nature 410, 974–979.

Moore, J.P., Kitchen, S.G., Pugach, P., Zack, J.A., 2004. The CCR5 and CXCR4 coreceptors – central to understanding the transmission and pathogenesis of human immunodeficiency virus type 1 infection. AIDS Res. Hum. Retroviruses 20, 111–126.

Nishimura, Y., Igarashi, T., Donau, O.K., Buckler-White, A., Buckler, C., Lafont, B.A., Goeken, R.M., Goldstein, S., Hirsch, V.M., Martin, M.A., 2004. Highly pathogenic SHIVs and SIVs target different $CD4^+$ T cell subsets in rhesus monkeys, explaining their divergent clinical courses. Proc. Natl. Acad. Sci. U. S. A. 101, 12324–12329.

O'Brien, W.A., Hartigan, P.M., Martin, D., Esinhart, J., Hill, A., Benoit, S., Rubin, M., Simberkoff, M.S., Hamilton, J.D., 1996. Changes in plasma HIV-1 RNA and $CD4^+$ lymphocyte counts and the risk of progression to AIDS. Veterans Affairs Cooperative Study Group on AIDS. N. Engl. J. Med. 334, 426–431.

Okoye, A., Meier-Schellersheim, M., Brenchley, J.M., Hagen, S.I., Walker, J.M., Rohankhedkar, M., Lum, R., Edgar, J.B., Planer, S.L., Legasse, A., Sylwester, A.W., Piatak Jr., M., Lifson, J.D., Maino, V.C., Sodora, D.L., Douek, D.C., Axthelm, M.K., Grossman, Z., Picker, L.J., 2007. Progressive $CD4^+$ central memory T cell decline results in $CD4^+$ effector memory insufficiency and overt disease in chronic SIV infection. J. Exp. Med. 204, 2171–2185.

Okuma, K., Tanaka, R., Ogura, T., Ito, M., Kumakura, S., Yanaka, M., Nishizawa, M., Sugiura, W., Yamamoto, N., Tanaka, Y., 2008. Interleukin-4-transgenic hu-PBL-SCID mice: a model for the screening of antiviral drugs and immunotherapeutic agents against X4 HIV-1 viruses. J. Infect. Dis. 197, 134–141.

Pedroza-Martins, L., Gurney, K.B., Torbett, B.E., Uittenbogaart, C.H., 1998. Differential tropism and replication kinetics of human immunodeficiency virus type 1 isolates in thymocytes: coreceptor expression allows viral entry, but productive infection of distinct subsets is determined at the postentry level. J. Virol. 72, 9441–9452.

Roeth, J.F., Collins, K.L., 2006. Human immunodeficiency virus type 1 Nef: adapting to intracellular trafficking pathways. Microbiol. Mol. Biol. Rev. 70, 548–563.

Sallusto, F., Geginat, J., Lanzavecchia, A., 2004. Central memory and effector memory T cell subsets: function, generation, and maintenance. Annu. Rev. Immunol. 22, 745–763.

Sato, K., Aoki, J., Misawa, N., Daikoku, E., Sano, K., Tanaka, Y., Koyanagi, Y., 2008. Modulation of human immunodeficiency virus type 1 infectivity through incorporation of tetraspanin proteins. J. Virol. 82, 1021–1033.

Schnittman, S.M., Denning, S.M., Greenhouse, J.J., Justement, J.S., Baseler, M., Kurtzberg, J., Haynes, B.F., Fauci, A.S., 1990. Evidence for susceptibility of intrathymic T-cell precursors and their progeny carrying T-cell antigen receptor phenotypes $TCR\alpha\beta^+$ and $TCR\gamma\delta^+$ to human immunodeficiency virus infection: a mechanism for $CD4^+$ (T4) lymphocyte depletion. Proc. Natl. Acad. Sci. U. S. A. 87, 7727–7731.

Sereti, I., Sklar, P., Ramchandani, M.S., Read, S.W., Aggarwal, V., Imamichi, H., Natarajan, V., Metcalf, J.A., Kovacs, J.A., Tavel, J., Davey, R.T., Dersimonian, R., Lane, H.C., 2007. $CD4^+$ T cell responses to interleukin-2 administration in HIV-infected patients are

directly related to the baseline level of immune activation. J. Infect Dis. 196, 677–683.
Stevenson, M., Stanwick, T.L., Dempsey, M.P., Lamonica, C.A., 1990. HIV-1 replication is controlled at the level of T cell activation and proviral integration. EMBO J. 9, 1551–1560.
Traggiai, E., Chicha, L., Mazzucchelli, L., Bronz, L., Piffaretti, J.C., Lanzavecchia, A., Manz, M.G., 2004. Development of a human adaptive immune system in cord blood cell-transplanted mice. Science 304, 104–107.
Vatakis, D.N., Bristol, G., Wilkinson, T.A., Chow, S.A., Zack, J.A., 2007. Immediate activation fails to rescue efficient human immunodeficiency virus replication in quiescent CD4$^+$ T cells. J. Virol. 81, 3574–3582.
Wilpshaar, J., Falkenburg, J.H., Tong, X., Noort, W.A., Breese, R., Heilman, D., Kanhai, H., Orschell-Traycoff, C.M., Srour, E.F., 2000. Similar repopulating capacity of mitotically active and resting umbilical cord blood CD34$^+$ cells in NOD/SCID mice. Blood 96, 2100–2107.
Ye, P., Kirschner, D.E., Kourtis, A.P., 2004. The thymus during HIV disease: role in pathogenesis and in immune recovery. Curr. HIV Res. 2, 177–183.
Zack, J.A., Arrigo, S.J., Weitsman, S.R., Go, A.S., Haislip, A., Chen, I.S., 1990. HIV-1 entry into quiescent primary lymphocytes: molecular analysis reveals a labile, latent viral structure. Cell 61, 213–222.
Zhang, Z., Schuler, T., Zupancic, M., Wietgrefe, S., Staskus, K.A., Reimann, K.A., Reinhart, T.A., Rogan, M., Cavert, W., Miller, C.J., Veazey, R.S., Notermans, D., Little, S., Danner, S.A., Richman, D.D., Havlir, D., Wong, J., Jordan, H.L., Schacker, T.W., Racz, P., Tenner-Racz, K., Letvin, N.L., Wolinsky, S., Haase, A.T., 1999. Sexual transmission and propagation of SIV and HIV in resting and activated CD4$^+$ T cells. Science 286, 1353–1357.
Zhang, Z.Q., Wietgrefe, S.W., Li, Q., Shore, M.D., Duan, L., Reilly, C., Lifson, J.D., Haase, A.T., 2004. Roles of substrate availability and infection of resting and activated CD4$^+$ T cells in transmission and acute simian immunodeficiency virus infection. Proc. Natl. Acad. Sci. U. S. A. 101, 5640–5645.

Retrovirology

BioMed Central

Short report

Open Access

Comparative study on the effect of human BST-2/Tetherin on HIV-1 release in cells of various species

Kei Sato[1], Seiji P Yamamoto[1,2], Naoko Misawa[1], Takeshi Yoshida[1], Takayuki Miyazawa[3] and Yoshio Koyanagi*[1]

Address: [1]Laboratory of Viral Pathogenesis, Institute for Virus Research, Kyoto University, Kyoto, Kyoto 606-8507, Japan, [2]Department of Molecular and Cellular Biology, Graduate School of Biostudies, Kyoto University, Kyoto, Kyoto 606-8501, Japan and [3]Laboratory of Viral Pathogenesis, Center for Emerging Virus Research, Institute for Virus Research, Kyoto University, Kyoto, Kyoto 606-8507, Japan

Email: Kei Sato - ksato@virus.kyoto-u.ac.jp; Seiji P Yamamoto - syamamot@virus.kyoto-u.ac.jp; Naoko Misawa - nmisawa@virus.kyoto-u.ac.jp; Takeshi Yoshida - tkyoshid@virus.kyoto-u.ac.jp; Takayuki Miyazawa - tmiyazaw@virus.kyoto-u.ac.jp; Yoshio Koyanagi* - ykoyanag@virus.kyoto-u.ac.jp

* Corresponding author

Published: 2 June 2009

Retrovirology 2009, **6**:53 doi:10.1186/1742-4690-6-53

Received: 3 February 2009
Accepted: 2 June 2009

This article is available from: http://www.retrovirology.com/content/6/1/53

Abstract

In this study, we first demonstrate that endogenous hBST-2 is predominantly expressed on the plasma membrane of a human T cell line, MT-4 cells, and that Vpu-deficient HIV-1 was less efficiently released than wild-type HIV-1 from MT-4 cells. In addition, surface hBST-2 was rapidly down-regulated in wild-type but not Vpu-deficient HIV-1-infected cells. This is a direct insight showing that provirus-encoded Vpu has the potential to down-regulate endogenous hBST-2 from the surface of HIV-1-infected T cells. Corresponding to previous reports, the aforementioned findings suggested that hBST-2 has the potential to suppress the release of Vpu-deficient HIV-1. However, the molecular mechanism(s) for tethering HIV-1 particles by hBST-2 remains unclear, and we speculated about the requirement for cellular co-factor(s) to trigger or assist its tethering ability. To explore this possibility, we utilize several cell lines derived from various species including human, AGM, dog, cat, rabbit, pig, mink, potoroo, and quail. We found that ectopic hBST-2 was efficiently expressed on the surface of all analyzed cells, and its expression suppressed the release of viral particles in a dose-dependent manner. These findings suggest that hBST-2 can tether HIV-1 particles without the need of additional co-factor(s) that may be expressed exclusively in primates, and thus, hBST-2 can also exert its function in many cells derived from a broad range of species. Interestingly, the suppressive effect of hBST-2 on HIV-1 release in Vero cells was much less pronounced than in the other examined cells despite the augmented surface expression of ectopic hBST-2 on Vero cells. Taken together, our findings suggest the existence of certain cell types in which hBST-2 cannot efficiently exert its inhibitory effect on virus release. The cell type-specific effect of hBST-2 may be critical to elucidate the mechanism of BST-2-dependent suppression of virus release.

Findings

To accomplish efficient release of HIV-1 particles, HIV-1 Vpu is required in certain cells (e.g., HeLa cells) but is dispensable in other cell types (e.g., HEK293 and Cos-7 cells) [1-3]. A previous report suggested that an inhibitory factor(s) for HIV-1 release is expressed in HeLa cells and the

effect is attenuated by Vpu [4]. Recently, Neil and colleagues identified the inhibitor, hBST-2 (also called CD317 or HM1.24), in HeLa cells, and referred to this protein as "Tetherin" [5]. They also showed that the inhibitory action of hBST-2 on HIV-1 particle release was antagonized by Vpu, and they concluded that hBST-2 functions by tethering HIV-1 particles to the cell surface [5]. In addition, Van Damme and colleagues demonstrated that Vpu down-regulates hBST-2 from the surface of HeLa cells [6]. On the other hand, Miyagi and colleagues have recently reported that Vpu augments HIV-1 release without down-regulating surface hBST-2 in CEMx174 and H9 cells [7]. Therefore, the relevance of surface hBST-2 down-regulation and the antagonistic action of Vpu on the tethering ability of hBST-2 remain unclear.

We first set out to analyze the level of endogenous hBST-2 expression in a T cell line (MT-4 cells) and compared this level to that found for adherent cell lines (HeLa and HEK293 cells). Although flow cytometry indicated that the level of surface hBST-2 on MT-4 cells was comparable to that expressed on HeLa cells, Western blotting indicated that the total amount of endogenous hBST-2 protein in HeLa cells was much more than the level found in MT-4 cells (Figures 1A–C). These results indicate that endogenous hBST-2 in MT-4 cells is predominantly expressed on the plasma membrane.

To analyze the sensitivity of endogenous hBST-2 on the surface of MT-4 cells to Vpu antagonism, MT-4 cells were infected with either wild-type or Vpu-deficient HIV-1, and the level of surface hBST-2 was subsequently monitored. The amount of released virions in the culture supernatant of wild-type HIV-1-infected cells was significantly higher when compared to that of Vpu-deleted HIV-1-infected cells (Figure 1E), while the percentage of p24-positive cells in wild-type HIV-1-infected culture was similar to that in Vpu-deleted HIV-1-infected culture (Figure 1F). These results suggest that the liberation of Vpu-deficient HIV-1 virions was impaired by endogenous hBST-2 in MT-4 cells. In addition, we clearly found that the surface expression of hBST-2 on wild-type but not Vpu-deleted HIV-1-infected cells (i.e., p24-positive cells) was severely down-regulated (Figures 1D and 1H). Although it has remained ambiguous in the literature whether endogenous hBST-2 on the surface of human T cells is down-regulated by HIV-1 infection [6,7], this is the first demonstration of the significant down-regulation of endogenous hBST-2 in T cells by Vpu which resulted from HIV-1 infection and not from transfection with a Vpu-expressing plasmid [6,8].

Following the rapid down-regulation of surface hBST-2 by infection with wild-type HIV-1, the surface expression of hBST-2 was gradually but significantly replenished along with HIV-1 expansion (Figures 1D and 1H). It is unclear how and why the surface levels of hBST-2 increased; however, our finding indicates that the level of down-regulation of surface hBST-2 on HIV-1-infected T cells would vary depending on the time after infection.

Consistent with previous reports, our findings suggested that hBST-2 has the potential to attenuate HIV-1 release [5,6]. However, how hBST-2 acts against the release of HIV-1 particles remains unclear, and it is not known whether the hBST-2 function involves additional cellular co-factor(s). Since the potential of hBST-2 for the suppression of HIV-1 release has been reported only in primate cell lines [5-7], we hypothesized that hBST-2 may utilize co-factor(s) expressed uniquely in primate cells to tether virions. To investigate the role of hBST-2, we set forward to use various cell lines derived from 9 animal species including human, AGM, dog, cat, rabbit, pig, mink, potoroo, and quail. These cells were transfected with either wild-type or Vpu-deficient HIV-1-producing plasmid (pNL4-3 or pNL43-Udel). The amounts of released virions from HEK293, Vero, Cos-7, D-17, PK-15, RSC, Mv.1.Lu, and QT6 cells were quantified by TZM-bl titration assay [9], while those from CRFK and PtK2 cells were quantified by p24 ELISA because of their lower infectivity [10] (Figure 2). As previously described [4-6,11], HeLa cells were incompetent for the release of Vpu-deficient HIV-1 (Figure 2). In contrast, the other cell lines examined here were able to produce almost comparable amounts of Vpu-deficient HIV-1 when compared to the release of wild-type HIV-1 (Figure 2). These results indicate the absence in these examined cells of intrinsic factors which have the potential to be similar to hBST-2 and can be antagonized by Vpu.

Previous studies have shown that rhTRIM5α, a well-known restriction factor for HIV-1 replication [12,13], is able to efficiently elicit its suppressive ability for HIV-1 replication in feline CRFK cells, but not in canine D-17 cells [14,15]. These results suggest the species-specific ability of rhTRIM5α to suppress HIV-1 replication. To investigate the species-specific tethering ability of hBST-2, we next co-transfected an hBST-2-expressing plasmid (phBST-2) with either pNL4-3 or pNL43-Udel in the above examined cell lines and harvested released virions at 24 hours post-transfection. As shown in Figure 2, exogenous hBST-2 in these cell lines clearly suppressed the release of Vpu-deficient HIV-1 in a dose-dependent manner. This result strongly indicates that hBST-2 can tether released HIV-1 particles without any other unidentified co-factors that are expressed exclusively in primates. It remains conceivable that hBST-2 could employ certain elements ubiquitously expressed in many species for the tethering of released virions. Although it has been controversial whether wild-type HIV-1 release can be suppressed

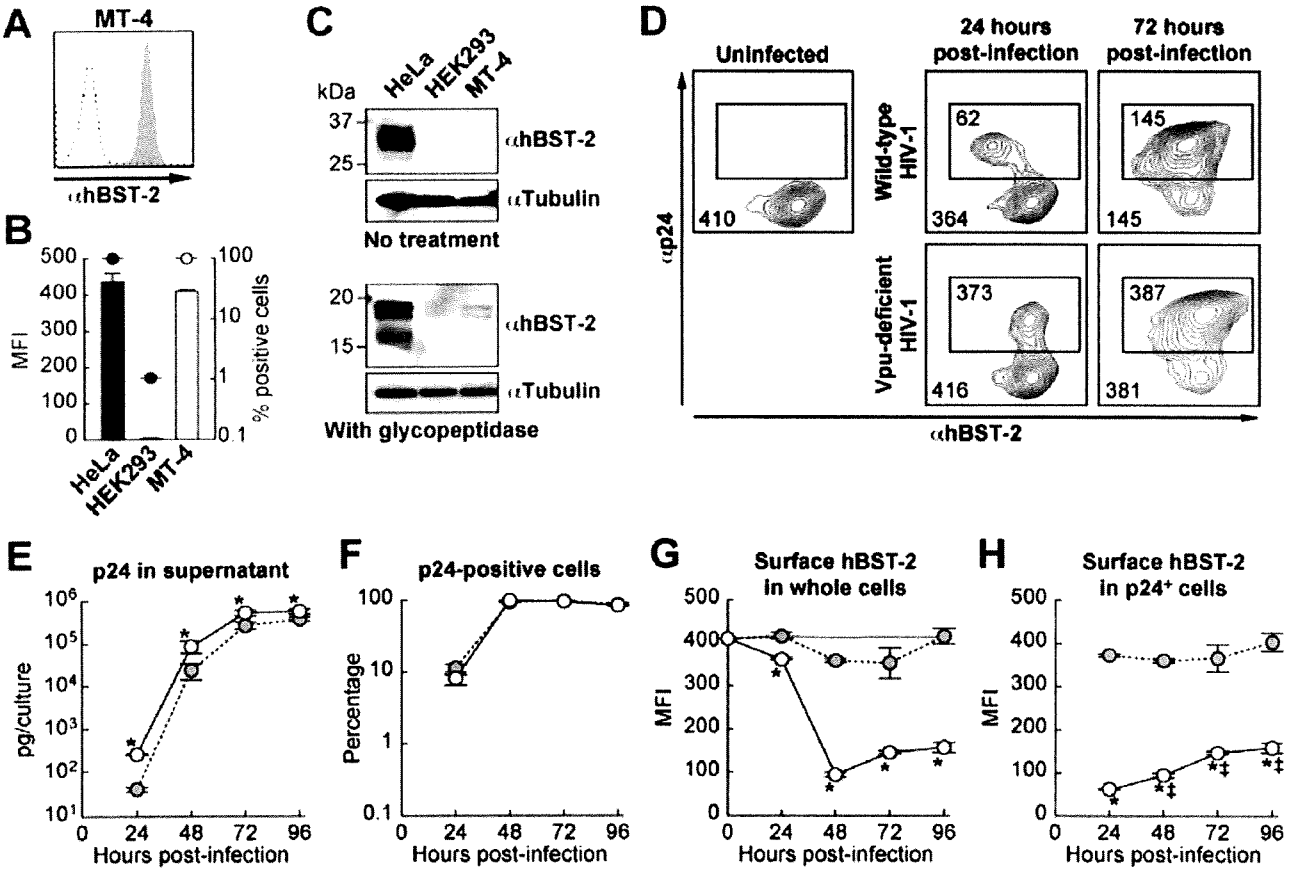

Figure 1

Sequential analysis on the level of endogenous hBST-2 on the surface of HIV-1-infected human T cells. (A and B) MT-4 cells were stained with a mouse anti-hBST-2 antibody, and the surface expression of endogenous hBST-2 (filled in gray) was analyzed by flow cytometry as described in the Materials and Methods. Isotype IgG was used as a negative control (broken line). A representative result (A) and summarized graph (B) are shown. The level of endogenous hBST-2 on the surface of MT-4 cells (opened bar and circle) is compared to that of HeLa and HEK293 cells (filled bars and circles). MFI is represented in bars (Y-axis on left), and the percentage of hBST-2-positive cells is represented in circles (Y-axis on right, log scale). (C) The level of endogenous hBST-2 expression in HeLa, HEK293, and MT-4 cells was analyzed by Western blotting (top panel). For clear detection of hBST-2, the cell lysates were treated with glycopeptidase as described in the Materials and Methods, and the level of deglycosylated hBST-2 was analysed by Western blotting (bottom panel). The input was standardized to Tubulin, and representative results are shown. kDa, kilodalton. (D-H) MT-4 cells were infected with either wild-type or Vpu-deficient HIV-1 (MOI 0.1). Endogenous hBST-2 on the cell surface and intracellular expression of p24 were sequentially analyzed by flow cytometry, and representative profiles are shown (D). The number in the corner of the plot indicates MFI of hBST-2 on the surface of whole cells, and that in the square in the plot indicates MFI of hBST-2 on the surface of p24-postive cells. The amount of p24 in the culture supernatant (E), the percentage of p24-positive cells (F), the level of hBST-2 on the surface of whole cells (G), and the level of hBST-2 on the surface of p24-positive cells (H) following infection with either wild-type (opened circles with line) or Vpu-deficient (filled circles in gray with broken line) HIV-1 were sequentially measured. The amount of p24 in the culture supernatant was quantified by p24 ELISA, and the other data were obtained by flow cytometry as described in the Materials and Methods. Gray line in panel G indicates MFI of surface hBST-2 on mock-infected cells. All experiments were performed in triplicate. Asterisks indicate statistical significance (Student's t test, $P < 0.05$) versus the values of Vpu-deficient HIV-1 at the same time point, and double daggers in panel H indicate statistical significance (Student's t test, $P < 0.05$) versus the values of wild-type HIV-1 at 24 hours post-infection. Error bars indicate standard deviations.

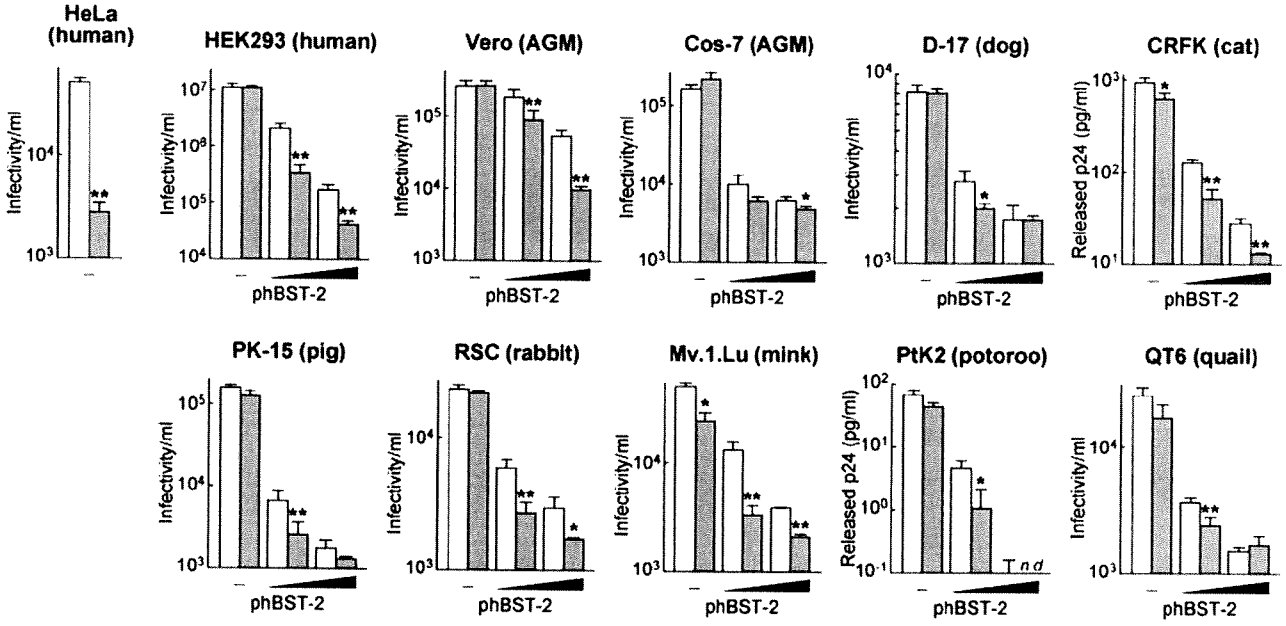

Figure 2

Suppression of HIV-1 release by exogenous hBST-2 in various cell lines. One microgram of pNL4-3 and pNL43-Udel was each co-transfected with (20 or 100 ng) or without (-) phBST-2 into several lines of cells as described in the Materials and Methods. The amount of wild-type (opened bars) or Vpu-deficient HIV-1 virion (bars filled in gray) released from HeLa, HEK293, Vero, Cos-7, D-17, PK-15, RSC, Mv.1.Lu, and QT6 was quantified by using TZM-bl cells, and the amount of HIV-1 released from CRFK and PtK2 cells was quantified by p24 ELISA. All experiments were performed in triplicate. Statistical significance (Student's *t* test) versus wild-type HIV-1 values is represented as follows: *, $P < 0.05$; **, $P < 0.01$. Error bars indicate standard deviations. *n.d.*, not detectable.

by ectopic hBST-2 or not [5,6], we observed here that the release of wild-type HIV-1 was attenuated by hBST-2 and that the efficiency of hBST-2 for the release of wild-type HIV-1 was significantly lower than that for the release of Vpu-deleted HIV-1 (Figure 2).

Ectopically expressed hBST-2 was detected on the surface of all cell lines used in this study (Figure 3A). Unexpectedly, we found the staining with this antibody in native AGM cell lines, Vero and Cos-7 cells (Figure 3A) that increased in intensity when treated with IFN-α (data not shown). It is known that hBST-2 expression is induced upon IFN-α treatment in HEK293 cells [5,6]. Therefore, the antibody-specific staining and its increased signal intensity that we observed in the AGM cells could be due to the cross-reactivity of the anti-BST-2 antibody with endogenous AGM BST-2.

As previously reported [6], we also found that endogenous hBST-2 on HeLa cells was significantly down-regulated by transfection with pNL4-3, but not with pNL43-Udel (Figure 3B). In contrast, at 24 hours post-transfection, the down-regulation of exogenous hBST-2 on the surface of the other cell lines was hardly observed except for Vero cells (Figure 3B). However, after 48 hours post-transfection, we could detect significant down-regulation of ectopically expressed hBST-2 on the surface of cells co-transfected with either pNL4-3 or a Vpu-expressing plasmid [8] (data not shown). These results suggest that the level of Vpu expression at 24 hours post-transfection is sufficient to antagonize the tethering ability of hBST-2, while not down-regulating surface hBST-2. In support of our data, a recent report showed that Vpu enhances HIV-1 release in the absence of surface down-regulation of hBST-2 [7]. Taken together, these results indicate that the down-regulation of surface hBST-2 may be dispensable for the antagonism of tethering ability of hBST-2 by Vpu.

We further assessed the results obtained from all the examined cell lines and focused on the correlation between the efficiency of particle release and the level of surface hBST-2 in these cells. All of the examined cell lines except for Vero cells showed significant suppression of virus release by exogenously expressed hBST-2 (Figure 4). In addition, a direct correlation between the suppression efficiency for virus release by hBST-2 and the level of surface hBST-2 was found in these cells with high correlation coefficients (Figure 4) and statistical significance ($P <$

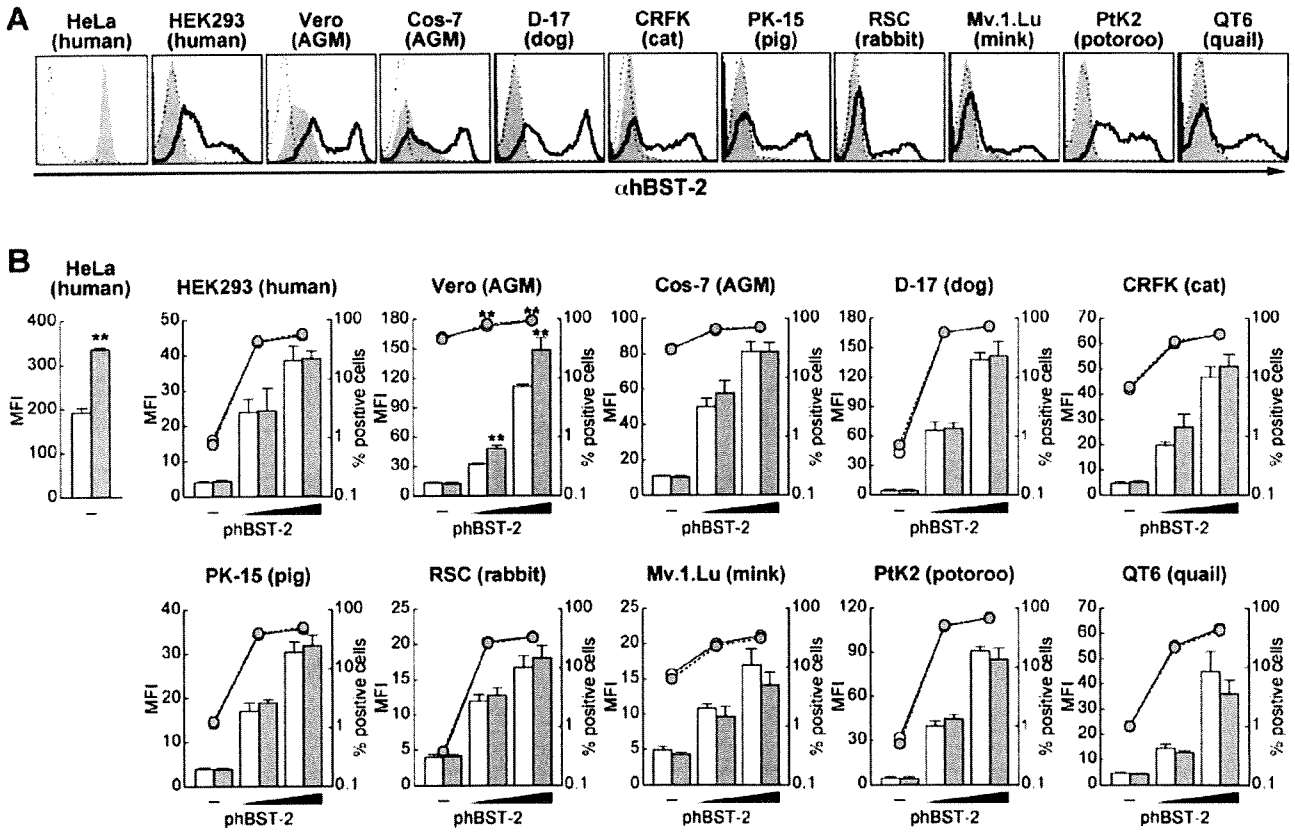

Figure 3

Surface expression of exogenous hBST-2 in various cell lines. (A) HEK293, Vero, Cos-7, D-17, CRFK, PK-15, RSC, Mv.1.Lu, PtK2, and QT6 cells were transiently transfected with 100 ng of phBST-2. phBST-2-transfected cells (black line) and mock-transfected cells (filled in gray) as well as HeLa cells (filled in gray) were stained with a mouse anti-hBST-2 monoclonal antibody, and the surface expression of hBST-2 was analyzed by flow cytometry as described in the Materials and Methods. Isotype IgG was used as a negative control (broken line). A representative result is shown. (B) One microgram of pNL4-3 and pNL43-Udel was each co-transfected with (20 or 100 ng) or without (-) phBST-2 into several lines of cells as described in Figure 2. The surface expression of hBST-2 on pNL4-3-co-transfected (opened bars and circles) and pNL43-Udel-co-transfected (gray bars and circles) cells was analyzed by flow cytometry. MFI is represented in bars (Y-axis on left), and the percentage of hBST-2-positive cells is represented in circles (Y-axis on right, log scale). All experiments were performed in triplicate. Statistical significance (Student's *t* test) versus wild-type HIV-1 values is represented as follows: *, $P < 0.05$; **, $P < 0.01$. Error bars indicate standard deviations.

0.01). On the other hand, the suppression efficiency for virus release by hBST-2 in Vero cells was relatively milder than in the other 9 cell lines even though Vero cells exhibited the highest levels of hBST-2 cell surface expression (Figure 4). Moreover, the result from Vero cells displayed a statistically different pattern than in the other cells (Figure 4, $P < 0.01$ by repeated measure ANOVA). These findings suggest that ectopic hBST-2 is unable to efficiently exert its inhibitory effect on virus release in Vero cells. One plausible explanation for this anomaly may be attributed to a defective IFN-α response. Although a previous study showed that the release of Vpu-deficient HIV-1 was suppressed upon IFN-α treatment [11], Vero cells are known to be genetically deficient in type I IFN genes, including IFN-α [16,17]. Therefore, it is conceivable that a signal cascade mediated by IFN-α may be needed to assist the tethering action of ectopic hBST-2, but that this cascade may not be operative in Vero cells because of its defects in type I IFN genes. Further studies in Vero cells will be needed to shed light on the unexplained aspects of the mechanism of suppression of virus release mediated by hBST-2.

It has recently been reported that hBST-2 has the potential to suppress the release of not only HIV-1 but also other retroviruses [18], Ebola virus [18], Lassa virus [19], and

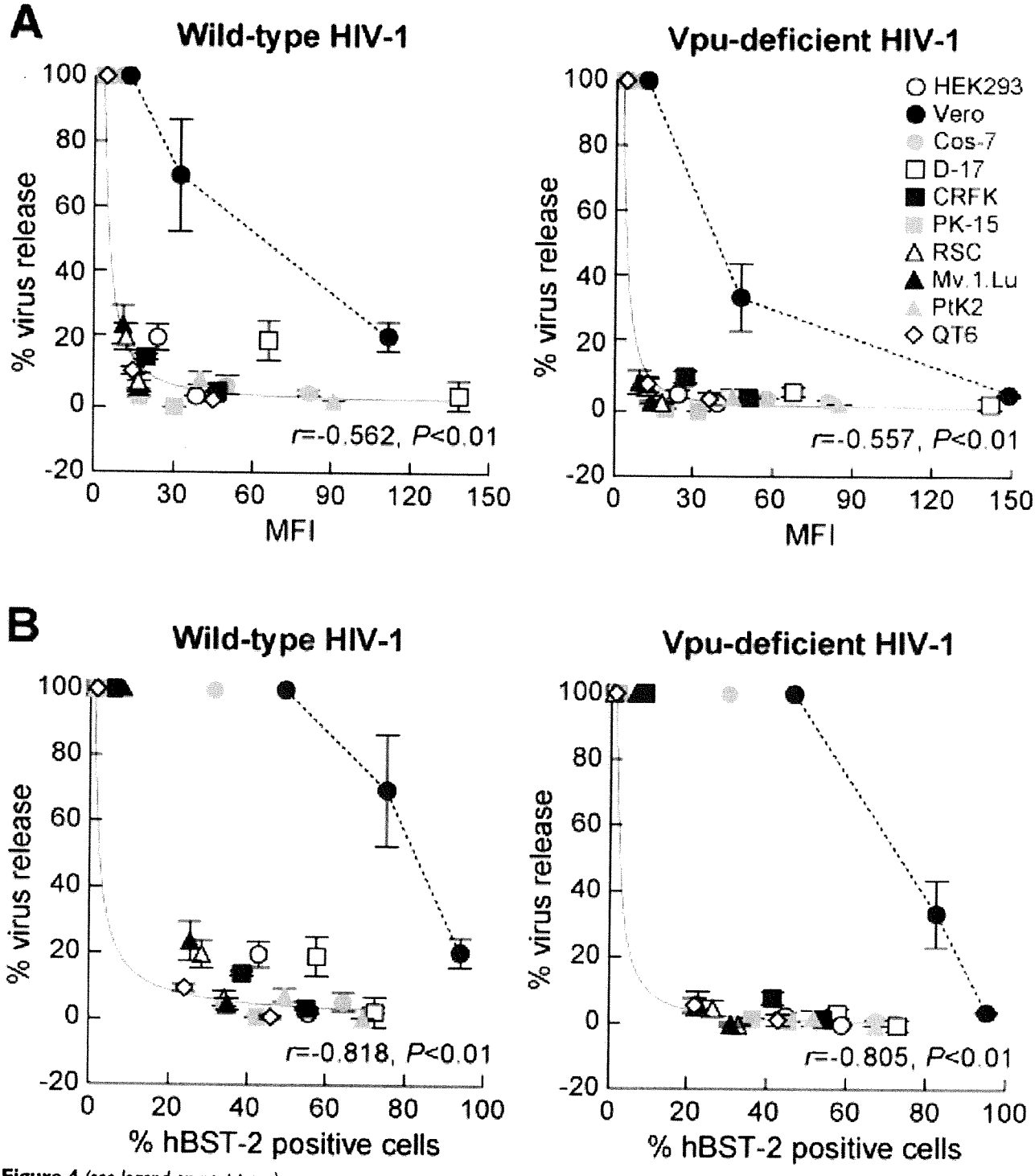

Figure 4 *(see legend on next page)*

Figure 4 *(see previous page)*
Comparison of the level of exogenous hBST-2 on plasma membrane with its inhibition efficiency for HIV-1 release in various cell lines. (A and B) The results shown in Figures 2 and 3 were summarized and rearranged as follows: the level of surface expression of hBST-2 is shown in MFI (A) and the percentage of surface hBST-2 positive cells (B) in the X-axis. To calculate % virus release (Y-axis), the infectivity of the culture supernatant of phBST-2-untransfected cells (for HEK293, Vero, Cos-7, D-17, RSC, Mv.1.Lu, and QT6 cells) or the amount of p24 in the culture supernatant of phBST-2-untransfected cells (for CRFK and PtK2) was defined as 100%. Statistical significance of the correlation between the level of surface hBST-2 (X-axis, shown in MFI or % positive cells) and % virus release (Y-axis) in the results from the 9 analyzed cells (HEK293, Cos-7, D-17, CRFK, PK-15, RSC, Mv.1.Lu, PtK2, and QT6 cells) was determined by Pearson's correlation test, and $P < 0.01$ was considered significant. Approximation curve of the result from the 9 analyzed cells is drawn in gray lines, and a representative result from Vero cells is drawn in broken line. *r*, Pearson's correlation coefficient.

Marburg virus [18,19]. Therefore, further studies on the mechanism of BST-2 function will provide beneficial information leading to novel therapeutic strategies against several virus-induced diseases including AIDS.

Methods

Cell culture

HEK293 cells (human kidney), Vero cells (AGM kidney), Cos-7 cells (AGM kidney), rabbit skin cells (RSC, kindly provided by Dr. B. Roizman), and TZM-bl cells (obtained from AIDS reagent program, National Institute of Health) were maintained in low-glucose DMEM (Nikken) containing 10% FCS and antibiotics. D-17 cells (canine osteosarcoma), CRFK cells (feline kidney), PK-15 cells (porcine kidney), Mv.1.Lu cells (*Mustela vison*, mink lung), and QT6 cells (*Coturnix coturnix japonica*, quail fibrosarcoma) were maintained in high-glucose DMEM (Sigma) containing 10% FCS, 2 mM GlutaMax (Invitrogen), and antibiotics. PtK2 cells (potoroo kidney) were maintained in Eagle's minimum essential medium (Sigma) supplemented with 1 mM sodium pyruvate, 2 mM GlutaMax, 10% FCS and antibiotics. MT-4 cells were maintained in RPMI1640 (Nikken) containing 10% FCS and antibiotics. Mv.1.Lu cells and QT6 cells were kindly donated by Dr. A. Koito.

Plasmid construction

To construct phBST-2, a *bst-2* cDNA (GenBank: NM_004335, bases 10-552) was amplified by polymerase chain reaction from a human leukocyte cDNA library (Invitrogen), and the resulting fragment was inserted into peGFP-C1 (Clontech). Sequence of the construct was confirmed with an ABI 3130xl genetic analyzer (Applied Biosystems).

Transfection and virus preparation

Cells were seeded in 6-well plate to appropriate densities 1-day prior to transfection and were transfected by using Lipofectamine 2000 reagent (Invitrogen) according to the manufacture's protocol. Briefly, 1 μg of pNL4-3 [20] or pNL43-Udel (kindly donated by Dr. K. Strebel) [1] was cotransfected with 20 or 100 ng of phBST-2. The amount of plasmid DNA for transfection was normalized to 2 μg per well. Four hour after transfection, culture medium was replaced freshly. The culture supernatant was harvested, centrifuged, and then filtrated with 0.45-μm filter (Millipore) to produce virus solutions at 24 hours post-transfection. All experiments were performed in triplicate. To prepare wild-type or Vpu-deficient HIV-1 for its infection assay, pNL4-3 or pNL43-Udel was transfected into HEK293 cells by the calcium phosphate method as previously described [21]. The prepared viruses were titrated by using peripheral blood mononuclear cells, and the $TCID_{50}$ was calculated as previously described [22].

TZM-bl assay

Quantification of the amount of released HIV-1 virion was performed by using TZM-bl cells as previously described [5]. Briefly, appropriate virus solution was inoculated into 1×10^5 TZM-bl cells per 12-well plate. The cells were harvested at 48 hours post-infection, and β-galactosidase assay was performed by using Galacto-Star Mammalian Reporter Gene Assay System (Applied Biosystems) according to the manufacture's procedure. Activity was measured with a 1420 ALBOSX multilabel counter (Perkin Elmer).

p24 ELISA

The amount of HIV-1 virion released from CRFK, PtK2, and MT-4 cells was quantified by using HIV-1 p24 ELISA kit (ZeptoMetrix) according to the manufacture's instructions.

Flow cytometry

Flow cytometry was performed as previously described [21]. A mouse anti-hBST-2 monoclonal antibody (donated by Chugai Pharmaceutical Co., Japan) [6,23] and a Cy5-conjugated donkey anti-mouse IgG antisera (Chemicon) were used. For costaining of cell surface hBST-2 and intracellular p24, the anti-hBST-2 monoclonal antibody was pre-labelled with Zenon Alexa Fluor 647 mouse IgG2a labelling kit (Invitrogen) according to the manufacture's protocol. Cell surface hBST-2 was stained with the pre-labelled anti-hBST-2 antibody, and

the cells were permeabiliezed and fixed with BD Cytoperm/Cytofix solution (BD Pharmingen). Then, intracellular p24 was stained with a FITC-conjugated anti-HIV-1 p24 antibody (clone 2C2, kindly provided by Dr. Y. Tanaka) [24].

Western blotting

Western blotting was performed as previously described [21] with some modification. Briefly, the cells were lysed with lysis buffer (1% NP-40, 50 mM Tris-HCl [pH7.5], 150 mM NaCl, 1 mM EDTA, 1 mM Na_3VO_4, and 1 mM PMSF). The lysates were separated by SDS-PAGE and transferred to Immobilon transfer membrane (Millipore). For detection, the mouse anti-hBST-2 monoclonal antibody, a mouse anti-Tubulin monoclonal antibody (clone DM1A; Sigma), and an HRP-conjugated horse anti-mouse IgG antibody (Cell Signalling) were used. It has been reported that hBST-2 is a highly glycosylated protein [25]. To remove the sugar chains in hBST-2 protein and detect hBST-2 more clearly, the lysates were treated with glycopeptidase F (TaKaRa) according to the manufacture's procedure.

Statistical analyses

Student's *t* test was used to determine statistical significance, and $P < 0.05$ and $P < 0.01$ were considered significant. The Pearson correlation coefficient was applied to determine statistical significance for the correlation between the suppression efficiency for particle release by hBST-2 and the level of surface hBST-2 in the 9 kinds of cells lines (Figure 4), and $P < 0.01$ was considered significant. Repeated measure ANOVA was applied to determine statistical significance between Vero cells and the other cell lines (Figure 4), and $P < 0.01$ was considered significant.

Abbreviations

h: human; BST-2: bone marrow stromal cell antigen-2; HIV-1: human immunodeficiency virus type 1; Vpu: viral protein U; AGM: African green monkey; ELISA: enzyme-linked immunosorbent assay; rhTRIM5α: rhesus macaque tripartite motif-containing 5 isoform α; phBST-2: hBST-2-expressing plasmid; IFN: interferon; AIDS: acquired immunodeficiency syndrome; DMEM: Dulbecco's modified Eagle medium; FCS: fatal calf serum; $TCID_{50}$: 50% tissue culture infectious dose; FITC: fluorescein isothiocyanate; EDTA: ethylenediaminetetraacetic acid; PMSF: phenylmethylsulfonyl fluoride; SDS-PAGE: sodium dodecyl sulfate-polyacrylamide gel electrophoresis; HRP: horseradish peroxidase; MOI: multiplicity of infection; MFI: mean fluorescence intensity.

Competing interests

The authors declare that they have no competing interests.

Authors' contributions

KS and YK designed the research; KS, SPY, NM, TM, and TY prepared the materials; KS, SPY, and NM performed the experiments and analyzed the obtained data; KS and SPY prepared the figures; KS, TM, and YK wrote the manuscript.

Acknowledgements

We thank Klaus Strebel (National Institute of Allergy and Infectious, Diseases, National Institutes of Health) for donating materials and helpful suggestions about this study, Atsushi Koito (Kumamoto University), Yuetsu Tanaka (University of the Ryukyus), and Bernard Roizman (The University of Chicago) for providing materials, Peter Gee, Takashi Fujita, Kazuhide Onoguchi, Takayuki Shojima (Institute for Virus Research, Kyoto University), and Shingo Iwami (Shizuoka University) for their generous help in this study. We also would like to express our appreciation for Ms. Kotubu Misawa's dedicated support. This work was supported by Grant-in-Aid for Scientific Research on Priority Areas from the Ministry of Education, Culture, Sports, Sciences, and Technology of Japan, and a Health and Labor Science Research Grant (Research on Publicly Essential Drugs and Medical Devices) from the Ministry of Health, Labor and Welfare of Japan and Japan Human Science Foundation. KS and TY were supported by Research Fellowships of the Japan Society for the Promotion of Science for Young Scientists. TM was supported by the Bio-oriented Technology Research Advancement Institution.

References

1. Klimkait T, Strebel K, Hoggan MD, Martin MA, Orenstein JM: **The human immunodeficiency virus type 1-specific protein vpu is required for efficient virus maturation and release.** *J Virol* 1990, **64**:621-629.
2. Nomaguchi M, Fujita M, Adachi A: **Role of HIV-1 Vpu protein for virus spread and pathogenesis.** *Microbes Infect* 2008, **10**:960-967.
3. Strebel K, Klimkait T, Martin MA: **A novel gene of HIV-1, vpu, and its 16-kilodalton product.** *Science* 1988, **241**:1221-1223.
4. Varthakavi V, Smith RM, Bour SP, Strebel K, Spearman P: **Viral protein U counteracts a human host cell restriction that inhibits HIV-1 particle production.** *Proc Natl Acad Sci USA* 2003, **100**:15154-15159.
5. Neil SJ, Zang T, Bieniasz PD: **Tetherin inhibits retrovirus release and is antagonized by HIV-1 Vpu.** *Nature* 2008, **451**:425-430.
6. Van Damme N, Goff D, Katsura C, Jorgenson RL, Mitchell R, Johnson MC, Stephens EB, Guatelli J: **The interferon-induced protein BST-2 restricts HIV-1 release and is downregulated from the cell surface by the viral Vpu protein.** *Cell Host Microbe* 2008, **3**:245-252.
7. Miyagi E, Andrew AJ, Kao S, Strebel K: **Vpu enhances HIV-1 virus release in the absence of Bst-2 cell surface down-modulation and intracellular depletion.** *Proc Natl Acad Sci USA* 2009, **106**:2868-2873.
8. Nguyen KL, llano M, Akari H, Miyagi E, Poeschla EM, Strebel K, Bour S: **Codon optimization of the HIV-1 vpu and vif genes stabilizes their mRNA and allows for highly efficient Rev-independent expression.** *Virology* 2004, **319**:163-175.
9. Koito A, Shigekane H, Matsushita S: **Ability of small animal cells to support the postintegration phase of human immunodeficiency virus type-1 replication.** *Virology* 2003, **305**:181-191.
10. Munk C, Zielonka J, Constabel H, Kloke BP, Rengstl B, Battenberg M, Bonci F, Pistello M, Lochelt M, Cichutek K: **Multiple restrictions of human immunodeficiency virus type 1 in feline cells.** *J Virol* 2007, **81**:7048-7060.
11. Neil SJ, Sandrin V, Sundquist WI, Bieniasz PD: **An interferon-α-induced tethering mechanism inhibits HIV-1 and Ebola virus particle release but is counteracted by the HIV-1 Vpu protein.** *Cell Host Microbe* 2007, **2**:193-203.
12. Stremlau M, Owens CM, Perron MJ, Kiessling M, Autissier P, Sodroski J: **The cytoplasmic body component TRIM5α restricts HIV-1 infection in Old World monkeys.** *Nature* 2004, **427**:848-853.

13. Sakuma R, Noser JA, Ohmine S, Ikeda Y: **Rhesus monkey TRIM5α restricts HIV-1 production through rapid degradation of viral Gag polyproteins.** *Nat Med* 2007, **13**:631-635.
14. Saenz DT, Teo W, Olsen JC, Poeschla EM: **Restriction of feline immunodeficiency virus by Ref1, Lv1, and primate TRIM5α proteins.** *J Virol* 2005, **79**:15175-15188.
15. Berube J, Bouchard A, Berthoux L: **Both TRIM5α and TRIMCyp have only weak antiviral activity in canine D17 cells.** *Retrovirology* 2007, **4**:68.
16. Emeny JM, Morgan MJ: **Regulation of the interferon system: evidence that Vero cells have a genetic defect in interferon production.** *J Gen Virol* 1979, **43**:247-252.
17. Mosca JD, Pitha PM: **Transcriptional and posttranscriptional regulation of exogenous human beta interferon gene in simian cells defective in interferon synthesis.** *Mol Cell Biol* 1986, **6**:2279-2283.
18. Jouvenet N, Neil SJ, Zhadina M, Zang T, Kratovac Z, Lee Y, McNatt M, Hatziioannou T, Bieniasz PD: **Broad-spectrum inhibition of retroviral and filoviral particle release by tetherin.** *J Virol* 2009, **83**:1837-1844.
19. Sakuma T, Noda T, Urata S, Kawaoka Y, Yasuda J: **Inhibition of Lassa and Marburg virus production by tetherin.** *J Virol* 2009, **83**:2382-2385.
20. Adachi A, Gendelman HE, Koenig S, Folks T, Willey R, Rabson A, Martin MA: **Production of acquired immunodeficiency syndrome-associated retrovirus in human and nonhuman cells transfected with an infectious molecular clone.** *J Virol* 1986, **59**:284-291.
21. Sato K, Aoki J, Misawa N, Daikoku E, Sano K, Tanaka Y, Koyanagi Y: **Modulation of human immunodeficiency virus type 1 infectivity through incorporation of tetraspanin proteins.** *J Virol* 2008, **82**:1021-1033.
22. Koyanagi Y, Tanaka Y, Kira J, Ito M, Hioki K, Misawa N, Kawano Y, Yamasaki K, Tanaka R, Suzuki Y, *et al.*: **Primary human immunodeficiency virus type 1 viremia and central nervous system invasion in a novel hu-PBL-immunodeficient mouse strain.** *J Virol* 1997, **71**:2417-2424.
23. Ohtomo T, Sugamata Y, Ozaki Y, Ono K, Yoshimura Y, Kawai S, Koishihara Y, Ozaki S, Kosaka M, Hirano T, Tsuchiya M: **Molecular cloning and characterization of a surface antigen preferentially overexpressed on multiple myeloma cells.** *Biochem Biophys Res Commun* 1999, **258**:583-591.
24. Okuma K, Tanaka R, Ogura T, Ito M, Kumakura S, Yanaka M, Nishizawa M, Sugiura W, Yamamoto N, Tanaka Y: **Interleukin-4-transgenic hu-PBL-SCID mice: a model for the screening of antiviral drugs and immunotherapeutic agents against X4 HIV-1 viruses.** *J Infect Dis* 2008, **197**:134-141.
25. Rollason R, Korolchuk V, Hamilton C, Schu P, Banting G: **Clathrin-mediated endocytosis of a lipid-raft-associated protein is mediated through a dual tyrosine motif.** *J Cell Sci* 2007, **120**:3850-3858.

Retrovirology

BioMed Central

Research

Open Access

MDM2 is a novel E3 ligase for HIV-1 Vif

Taisuke Izumi[1], Akifumi Takaori-Kondo*[1], Kotaro Shirakawa[1,2], Hiroaki Higashitsuji[3], Katsuhiko Itoh[3], Katsuhiro Io[1], Masashi Matsui[1], Kazuhiro Iwai[4,5], Hiroshi Kondoh[6], Toshihiro Sato[7], Mitsunori Tomonaga[7], Satoru Ikeda[7], Hirofumi Akari[8], Yoshio Koyanagi[9], Jun Fujita[3] and Takashi Uchiyama[1]

Address: [1]Department of Hematology and Oncology, Graduate School of Medicine, Kyoto University, 54 Shogoin-Kawaracho, Sakyo-ku, Kyoto 606-8507, Japan, [2]Japanese Foundation for AIDS Prevention, 1-3-12 Misaki-cho, Chiyoda-ku, Tokyo 101-0061, Japan, [3]Department of Clinical Molecular Biology, Graduate School of Medicine, Kyoto University, 54 Shogoin-Kawaracho, Sakyo-ku, Kyoto 606-8507, Japan, [4]Department of Molecular Cell Biology, Graduate School of Medicine, Osaka City University, 1-4-3 Asahi-machi, Abeno-ku, Osaka 545-8585, Japan, [5]CREST, Japan Science Technology Corporation, Kawaguchi, Saitama 332-0012, Japan, [6]Department of Geriatric Medicine, Graduate School of Medicine, Kyoto University, 54 Shogoin-Kawaracho, Sakyo-ku, Kyoto 606-8507, Japan, [7]Central Pharmaceutical Research Institute, Japan Tobacco Inc., 1-1 Murasaki-cho, Takatsuki, Osaka 569-1125, Japan, [8]Laboratory of Disease Control, Tukuba Primate Research Center, National Institute of Biomedical Innovation, Hachimandai-1, Tsukuba, Ibaraki 305-0843, Japan and [9]Laboratory of Viral Pathgenesis, Institute for Virus Research, Kyoto University, 53 Shogoin-Kawaracho, Sakyo-ku, Kyoto 606-8507, Japan

Email: Taisuke Izumi - izumi.t@aw3.ecs.kyoto-u.ac.jp; Akifumi Takaori-Kondo* - atakaori@kuhp.kyoto-u.ac.jp; Kotaro Shirakawa - kotash@kuhp.kyoto-u.ac.jp; Hiroaki Higashitsuji - hhigashi@virus.kyoto-u.ac.jp; Katsuhiko Itoh - katsu@virus.kyoto-u.ac.jp; Katsuhiro Io - katsu829@kuhp.kyoto-u.ac.jp; Masashi Matsui - mmatsui@kuhp.kyoto-u.ac.jp; Kazuhiro Iwai - kiwai@cellbio.med.osaka-u.ac.jp; Hiroshi Kondoh - hkondoh@kuhp.kyoto-u.ac.jp; Toshihiro Sato - toshihiro.sato@ims.jti.co.jp; Mitsunori Tomonaga - mitsunori.tomonaga@ims.jti.co.jp; Satoru Ikeda - satoru.ikeda@ims.jti.co.jp; Hirofumi Akari - akari@nibio.go.jp; Yoshio Koyanagi - ykoyanag@virus.kyoto-u.ac.jp; Jun Fujita - jfujita@virus.kyoto-u.ac.jp; Takashi Uchiyama - uchiyata@kuhp.kyoto-u.ac.jp

* Corresponding author

Published: 7 January 2009

Retrovirology 2009, **6**:1 doi:10.1186/1742-4690-6-1

Received: 16 September 2008
Accepted: 7 January 2009

This article is available from: http://www.retrovirology.com/content/6/1/1

Abstract

The human immunodeficiency virus type 1 (HIV-1) Vif plays a crucial role in the viral life cycle by antagonizing a host restriction factor APOBEC3G (A3G). Vif interacts with A3G and induces its polyubiquitination and subsequent degradation via the formation of active ubiquitin ligase (E3) complex with Cullin5-ElonginB/C. Although Vif itself is also ubiquitinated and degraded rapidly in infected cells, precise roles and mechanisms of Vif ubiquitination are largely unknown. Here we report that MDM2, known as an E3 ligase for p53, is a novel E3 ligase for Vif and induces polyubiquitination and degradation of Vif. We also show the mechanisms by which MDM2 only targets Vif, but not A3G that binds to Vif. MDM2 reduces cellular Vif levels and reversely increases A3G levels, because the interaction between MDM2 and Vif precludes A3G from binding to Vif. Furthermore, we demonstrate that MDM2 negatively regulates HIV-1 replication in non-permissive target cells through Vif degradation. These data suggest that MDM2 is a regulator of HIV-1 replication and might be a novel therapeutic target for anti-HIV-1 drug.

Background

Host restriction factors protect hosts from viruses, whereas viruses evade these proteins to replicate more efficiently in host cells. The interplay between the host restriction factors and viral proteins is therefore very important for regulating viral replication [1,2]. A3G (Apolipoprotein B mRNA editing enzyme, catalytic polypeptide-like 3G) is a newly identified anti-HIV-1 host factor [3], which belongs to the APOBEC superfamily of cytidine deaminases, consisting of APOBEC1, APOBEC2, AID (activation-induced cytidine deaminase), APOBEC3(A-H), and APOBEC4 [4]. A3G is incorporated into HIV-1 virions and inhibits HIV-1 replication by inducing G-to-A hypermutation in viral cDNA during reverse transcription [5-8]. HIV-1 Vif counteracts A3G by targeting it for proteasomal degradation, thus supporting HIV-1 replication in non-permissive target cells [9-11]. Vif forms a ubiquitin ligase (E3) complex with Cullin5 (Cul5), Elongin B, and Elongin C and functions as a substrate recognition subunit of this complex to induce ubiquitination and subsequent degradation of A3G [12,13]. Vif also counteracts several APOBEC3 proteins including APOBEC3F (A3F) [14,15]. These observations reconcile the long-standing mystery of why Vif function is necessary for HIV-1 to infect non-permissive cells. On the other hand, it has been shown that intracellular levels of Vif are maintained relatively low by ubiquitination in virus-producing cells [16-18]. Although several groups have reported E3 ligases important for Vif ubiquitination [17,18], the precise roles and mechanisms of Vif ubiquitination remain unclear. Here we demonstrate that MDM2 is a novel E3 ligase for Vif and that it induces ubiquitination and degradation of Vif, thereby regulating HIV-1 replication.

Results

MDM2 downregulates cellular Vif levels by inducing its degradation in a proteasome-dependent manner

To investigate the biological roles and molecular mechanisms of Vif ubiquitination, we tried to identify a novel E3 ligase that may be involved in the ubiquitination of Vif. During a search for Vif-interacting proteins in the HIV, Human Protein Interaction Database of National Institute for Allergy & Infectious Diseases http://www.ncbi.nlm.nih.gov/RefSeq/HIVInteractions/, we were struck by a protein called Gankyrin (proteasome 26S subunit, non-ATPase, 10 (PSMD10)). We first examined the biological effects of Gankyrin, but could not detect a downregulation of Vif (data not shown). As we previously reported that Gankyrin itself doesn't have an enzymatic activity and that it rather enhances the E3 ligase activity of MDM2 on p53 ubiquitination and degradation as a co-factor [19], we tested the possibility that MDM2 plays an important role in Vif ubiquitination as a novel E3 ligase. We examined the effect of several E3 ligases including MDM2 (a RING finger type E3 that mediates p53 ubiquitination and degradation [20]), Cul5 (another RING finger type E3 that forms a complex with Vif and is reported to induce Vif ubiquitination [17,21]), and Parkin (another RING finger type E3) on cellular Vif levels (Fig. 1A). HEK293T cells were transfected with a subgenomic expression vector pNL-A1 that expressed all HIV-1 proteins except for *gag* and *pol* products [22], together with the expression plasmids for these E3 ligases. We found that the ectopic expression of MDM2 downregulated the cellular levels of Vif as well as p53 in transfected cells in a dose-dependent manner (Fig. 1A, lanes 8–10), whereas Parkin and Cul5 did not affect their cellular levels (lanes 2–4 and 5–7, respectively), even though the latter proteins were expressed more than MDM2. Our results are discrepant with previous reports that demonstrated Cul5 induced Vif ubiquitination and degradation [17,23]. We assume that overexpression of Cul5 alone is insufficient to induce Vif degradation, because other E3 components are not overexpressed. Ectopic expression of MDM2 did not affect cellular levels of another viral protein such as Nef, suggesting that MDM2 specifically downregulated Vif levels; this result also excluded the possibility that MDM2 affected the transcriptional activity of the HIV-1 LTR.

Because it is well known that MDM2 regulates p53 levels by modulating its protein stability, we next examined the protein stability of Vif with the ectopic expression of MDM2. HEK293T cells were transfected with pNL-A1 with or without a MDM2 expression vector and treated with cycloheximide 21 hrs after transfection. After cycloheximide treatment, cellular levels of Vif decreased by 60% in MDM2-transfected cells and by 20% in control cells, respectively (Fig. 1B &1C), indicating that Vif decayed much faster when MDM2 was overexpressed. The stability profile of Vif protein was similar to that of p53 (Fig. 1B). However, in our hands, the half-life of Vif protein was longer than those shown in previous studies from several laboratories. We interpret that this difference is attributable to divergent methods used in the studies which employed radioisotopes or cycloheximide. Thus, our findings suggest that MDM2 affects the stability of Vif protein similar to its effect on p53. We also examined the stability of Vif in MDM2-/- MEF cells. Vif decayed much faster in p53-/- MEF cells than in p53-/-MDM2-/- double knock-out (DKO) MEF cells (Additional file 1), suggesting that endogenous MDM2 can also influence the stability of Vif. We then tested a RING finger domain-deleted MDM2 mutant, ΔRF, which is inactive for the ubiquitination activity of MDM2 [24]. Ectopic expression of MDM2 suppressed cellular Vif levels, but the expression of ΔRF did not (Fig. 1D). This result suggests that ubiquitination of Vif by MDM2 is involved in the downregulation of cellular Vif levels. We further treated transfected cells with a proteasome inhibitor MG132 to see whether the down-